

COMBINATION OF DONOR CHARACTERS IN DONOR-ACCEPTOR-
DONOR TYPE POLYMERS CONTAINING BENZOTHIADIAZOLE AND
QUINOXALINE AS THE ACCEPTOR UNITS

A THESIS SUBMITTED TO
THE GRADUATE SCHOOL OF NATURAL AND APPLIED SCIENCES
OF
MIDDLE EAST TECHNICAL UNIVERSITY

BY

MERVE ŞENDUR

IN PARTIAL FULFILLMENT OF THE REQUIREMENTS
FOR
THE DEGREE OF MASTER OF SCIENCE
IN
CHEMISTRY

DECEMBER 2011

Approval of the thesis:

COMBINATION OF DONOR CHARACTERS IN DONOR-ACCEPTOR-DONOR TYPE POLYMERS CONTAINING BENZOTHIADIAZOLE AND QUINOXALINE AS THE ACCEPTOR UNITS

submitted by **MERVE ŞENDUR** in partial fulfillment of the requirements for the degree of **Master of Science in Chemistry Department, Middle East Technical University** by,

Prof. Dr. Canan Özgen
Dean, Graduate School of **Natural and Applied Sciences** _____

Prof. Dr. İlker Özkan
Head of Department, **Chemistry** _____

Prof. Dr. Levent Toppare
Supervisor, **Chemistry Dept., METU** _____

Examining Committee Members:

Prof. Dr. Erdal Bayramlı
Chemistry Dept., METU _____

Prof. Dr. Levent Toppare
Chemistry Dept., METU _____

Prof. Dr. Teoman Tinçer
Chemistry Dept., METU _____

Assoc. Prof. Dr. Ali Çırpan
Chemistry Dept., METU _____

Assoc. Prof. Dr. Metin Ak
Chemistry Dept., Pamukkale University _____

Date: 30.12.2011

I hereby declare that all information in this document has been obtained and presented in accordance with academic rules and ethical conduct. I also declare that, as required by these rules and conduct, I have fully cited and referenced all material and results that are not original to this work.

Name, Last Name: MERVE ŞENDUR

Signature

ABSTRACT

COMBINATION OF DONOR CHARACTERS IN DONOR-ACCEPTOR-DONOR TYPE POLYMERS CONTAINING BENZOTHIADIAZOLE AND QUINOXALINE AS THE ACCEPTOR UNITS

Şendur, Merve

M. Sc., Department of Chemistry

Supervisor: Prof. Dr. Levent Toppare

December 2011, 73 pages

Donor-acceptor-donor approach is one of the effective ways to synthesize low band gap polymers. The monomers that will be designed with respect to donor-acceptor-donor approach have low band gap achieved by the coupling of a strong donor with high HOMO level to a strong acceptor with low LUMO level. Thus, the new donor-acceptor material will have a reduced bandgap (E_g) relative to either of its parent components. Due to this point of view, in this study, new electroactive benzothiadiazole and 2,3-bis(4-(tert-butyl)phenyl)quinoxaline monomers substituted with different donor groups (3,4-ethylenedioxythiophene and thiophene) were synthesized to explain the effect of different donor groups on the electronic and optical properties of DAD type polymers. The characterizations of the monomers were performed by ^1H and ^{13}C NMR techniques. Electrochemical behavior of both monomers and polymers were

studied by cyclic voltammetry. The electrochromic properties of the synthesized conducting polymers were investigated by several methods like spectroelectrochemistry, kinetic and colorimetry studies. The polymers having two different donor units may behave as a copolymer of the symmetric monomer having the same donor groups. Hence, the properties of copolymers were investigated with the co-monomers having either thiophene or 3,4-ethylenedioxythiophene as the donor group.

Keywords: Benzothiadiazole, Quinoxaline, Donor-Acceptor-Donor Theory, Electrochromism, Donor Effect.

ÖZ

FARKLI DONÖR GRUPLARININ DONÖR-AKSEPTÖR-DONÖR TİPİ BENZOTİYADİAZOL VE KİNOKSALİN İÇERİKLİ POLİMERLER ÜZERİNE ETKİLERİ

Şendur, Merve

Yüksek Lisans, Kimya Bölümü

Tez Yöneticisi: Prof. Dr. Levent Toppare

Aralık 2011, 73 sayfa

Donör-akseptör-donör yaklaşımı düşük bant aralığına sahip polimerlerin sentezlemenin etkili yollarından biridir. Donör-akseptör-donör yaklaşımıyla sentezlenen monomerler, yüksek HOMO düzeyine sahip donör ile düşük LUMO düzeyine sahip akseptörün birleşimiyle düşük bant aralığına sahip olurlar. Bu nedenle, yeni donör-akseptör polimer, esas bileşenlerinin herhangi birine göre daha düşük bir bant aralığına sahip olur. Bu bakımdan, bu çalışmada, yeni elektroaktif, farklı donör gruplar içeren benzotiyadiazol ve kinoksalin monomerleri sentezlenerek farklı donör grupların donör-akseptör-donör tipi polimerlerin elektronik ve optik özelliklerine etkileri incelenmiştir. Elde edilen monomerler ^1H ve ^{13}C NMR gibi teknikler kullanılarak karakterize edilmiştir. Monomerlerin ve elektrokimyasal sentezlenen iletken polimerlerin elektrokimyasal davranışları, dönüşümlü voltametri ile çalışılmıştır. Ayrıca polimerlerin elektrokromik özellikleri; spektroeletrokimyasal, kinetik ve kolorimetrik

alıřmalar gibi deęiřik metotlarla arařtırılmıřtır. Farklı iki donör grubu ieren polimerlerin, tek tip donör grubu ieren polimer eřlerinin kopolimeri gibi davranabileceęini göz önüne alarak tek tip donör grubu ieren polimer eřlerinin kopolimerizasyonu ve özellikleri incelenmiřtir.

Anahtar kelimeler: Benzotiyadiazol, Kinoksalin, Donör-Akseptör-Donör Teori, Elektrokromizm, Donör Etkisi.

To My Beloved Nephews

ACKNOWLEDGMENTS

I would like to express my gratitude to my supervisor Prof. Dr. Levent Toppare for their guidance, support, advice, criticism and most importantly being a hero model for me.

Abidin Balan and Derya Baran; my bosses, my teachers, my siblings and my friends, beyond for everything they done, create a family in the lab.

I would like to reveal my appreciation to Betül Cengiz to her priceless friendship. I would be not possible to endure all the things I have been through during undergraduation and graduation years without her.

Special thanks to my second family; Ruba İzzet-Tatar, Nimet İlkem Evcimen, Seher Peykari, İlhan Şen, Hilal Tutumlu, Ali Baykara, Ufuk Büyükaşahin and Baki Emre Çetindağ (in Ankara) and Tuğçe Gönül, Berkay Yıldırım, Banu Arslan, Zeynel Abidin Burak, Kürşat Demirel and Gözde Yıldız (in İstanbul) for their kind friendships, happiness and joy I felt when they were with me and bearing my all grouch.

Many thanks to all Toppare Research Group members for their kind friendships and supports.

Words fail to express my eternal gratitude to my spiritual mother, Deniz İlginer, for everything she has done for me. There is no another mother like her and there will be not to me.

Can Şendur and Doruk Ilginer for being such adorable nephews and their matured characters to understand why I had to work so hard instead of being with them to play.

Finally, I would like to present my greatest appreciation to Memet Hayrettin Şendur, for the sacrifices he has done during my university years and being my daddy.

TABLE OF CONTENTS

ABSTRACT	iv
ÖZ.....	vi
ACKNOWLEDGMENTS.....	ix
LIST OF TABLES	xiv
LIST OF FIGURES.....	xv
ABBREVIATIONS	xix
1. INTRODUCTION.....	1
1.1 Conjugated Polymers	1
1.2 Electrochromism	3
1.2.1 Electrochromism in Conducting Polymers	5
1.3 Band Gap Theory	7
1.3.1 Factors Affecting the Band Gap.....	9
1.3.2 Donor-Acceptor Theory	11
1.4 Electrochemical Doping Process in Conducting Polymers.....	13
1.5 Polymerization Methods	15
1.5.1 Electrochemical Polymerization	15
1.6 Characterization of Electrochromic Polymers	18
1.6.1 Cyclic Voltammetry (CV).....	18
1.6.2 Spectroelectrochemistry.....	19
1.6.3 Kinetic Studies	20
1.7 Aim of This Study.....	21
2. EXPERIMENTAL	22
2.1 Materials.....	22
2.2 Equipments.....	23
2.3 Synthesis of Monomers.....	24

2.3.1	Synthesis of 4-bromo-7-(2,3-dihydrothieno[3,4-b][1,4]dioxin-5-yl)benzo[c][1,2,5]thiadiazole	24
2.3.2	Synthesis of 4-(2,3-dihydrothieno[3,4-b][1,4]dioxin-5-yl)-7-(thiophen-2-yl)benzo[c][1,2,5]thiadiazole (EBT)	25
2.3.3	Synthesis of 2,3-Bis(4-tert-butylphenyl)-5,8-di(thiophen-2-yl)quinoxaline (TQT) and 5-Bromo-2,3-bis(4-tert-butylphenyl)-8-(thiophen-2-yl)quinoxaline (1)	26
2.3.4	Synthesis of 2,3-Bis(4-tert-butylphenyl)-5-(2,3-dihydrothieno[3,4-b][1,4]dioxin-5-yl)-8-(thiophen-2-yl)quinoxaline (EQT)	28
2.4	Synthesis of the Polymers	29
2.4.1	Homopolymerization of EBT	29
2.4.2	Copolymerization of TBT and EBE	29
2.4.3	Homopolymerization of TQT and EQT	30
3.	RESULTS AND DISCUSSION	33
3.1	Electrochemical and Optical Properties of Benzothiadiazole Derivative Homo- and Co-polymers	33
3.1.1	Electrochemical and Optical Properties of PEBT	33
3.1.1.1	Electrochemistry of PEBT	33
3.1.1.2	Optical Properties of P ₃	36
3.1.2	Comparison of PEBT with Its Homologous PTBT and PEBE	40
3.1.3	Electronic and Optical Properties of Copolymers	43
3.1.3.1	Electrochemical Studies of Copolymers	43
3.1.3.2	Spectroelectrochemical Studies of Copolymers and Comparison with Homopolymers	45
3.2	Electrochemical and Optical Properties of Quinoxaline Derivative Polymers	48
3.2.1	Electrochemical and Optical Properties of PTQT and PEQT	48
3.2.1.1	Electrochemistry of PTQT and PEQT	48
3.2.1.2	Optical Studies of PTBPTQ and PTBPETQ	51
4.	CONCLUSION	56
	REFERENCES	57

APPENDICES.....	60
A. NMR DATA.....	60
B. HRMS DATA.....	69
C. CYCLIC VOLTAMMOGRAMS OF COPOLYMERS.....	70

LIST OF TABLES

TABLES

Table 3 1 Electronic and optical results for PTBT, PEBE and PEBT.	42
Table 3 2 Monomer oxidation and accompanied polymer redox potentials of copolymers prepared from co-monomers TBT and EBE.....	44
Table 3 3 Maximum wavelength values and optical band gap energies of PTBT, PEBE, PEBT and resulting copolymers.....	47
Table 3 4 Monomer Oxidation, Corresponding Polymer Redox Potentials, Band Energies (HOMO/LUMO values), Optical and Electronic Bandgap Values of PTQT, PEQT, and PEQE	51

LIST OF FIGURES

FIGURES

Figure 1.1 Some examples of first and second generation conducting polymers	2
Figure 1.2 Molecular structures of some of the third generation conducting homo- and co- polymers.	3
Figure 1.3 Molecular structures of viologens and their different redox states.....	5
Figure 1.4 One of the examples on electrochromic display device application of conducting polymers	6
Figure 1.5 Energy level differences of insulator, semiconductor and metal.	8
Figure 1.6 Schematic representation of factors affecting E_g	9
Figure 1.7 Summary of the methodologies using for lowering the band gap	12
Figure 1.8 Schematic representation of band gap lowering by using different donor units coupling with same acceptor unit.	13
Figure 1.9 Charge carriers in PPy and its corresponding energy bands.....	15
Figure 1.10 Schematic representation of electropolymerization mechanisms of heterocycles (X = S, O, NH)	17
Figure 1.11 Cyclic voltammetry waveform and cyclic voltammogram for a reversible redox reaction.	18
Figure 1.12 1) Structure of mostly used electrochromic polymer; PEDOT and 2) colors of PEDOT in its reduced and oxidized state with its spectra.	20
Figure 2.1 Synthetic route for 4-bromo-7-(2,3-dihydrothieno[3,4-b][1,4]dioxin-5-yl)benzo[c][1,2,5]thiadiazole	24
Figure 2.2 Synthetic route for 4-(2,3-dihydrothieno[3,4-b][1,4]dioxin-5-yl)-7-(thiophen-2-yl)benzo[c][1,2,5]thiadiazole (EBT).....	25

Figure 2.3 Synthetic pathway for 2,3-bis(4-tert-butylphenyl)-5,8-di(thiophen-2-yl)quinoxaline (TQT) and 5-bromo-2,3-bis(4-tert-butylphenyl)-8-(thiophen-2-yl)quinoxaline (1).....	26
Figure 2.4 Synthetic route for 2,3-Bis(4-tert-butylphenyl)-5-(2,3-dihydrothieno[3,4-b][1,4]dioxin-5-yl)-8-(thiophen-2-yl)quinoxaline EQT.....	28
Figure 2.5 Structural representations of electrochemical copolymers	30
Figure 2.6 Chemical structures of benzothiadiazole bearing monomers and their corresponding polymers	31
Figure 2.7 Chemical structures of quinoxaline bearing monomers and their corresponding polymers	32
Figure 3.1 Electrochemical deposition of PEBT on ITO-coated glass slide in a 0.1 M DCM/ACN/TBAPF ₆ solvent-electrolyte couple.....	34
Figure 3.2 p- and n-doping of PEBT.....	35
Figure 3.3 Scan rate dependence of PEBT film for p-doping in 0.1 M ACN/TBAPF ₆ solvent-electrolyte couple at 100, 150, 200, 250, 300, 350 and 400 mV.s ⁻¹	36
Figure 3.4 Electronic absorption spectra of PEBT in 0.1 M ACN/TBAPF ₆ system upon p-type doping process.....	37
Figure 3.5 Optical changes of P ₃ in neutral, p- and n- doped states.....	39
Figure 3.6 Optical transmittance changes of PEBT at 408 nm, 620 nm and 1050 nm in 0.1 M ACN/TBAPF ₆ system while switching the potentials between its neutral. 40 and oxidized states	40
Figure 3.7 First cycles of TBT, EBE and EBT in 0.1 M DCM/ACN/TBAPF ₆ solvent-electrolyte couple during electrochemical polymerization	41
Figure 3.8 Electronic absorption spectra of monomers TBT, EBE and EBT (left) in CHCl ₃ and polymers PTBT, PEBE and PEBT in thin film form (right).	43
Figure 3.9 Normalized absorbance spectra of PTBT, PEBE, PEBT and the copolymer films prepared from different compositions (all in neutral state).	46
Figure 3.10 Electrochemical deposition of PTQT (a) and PEQT (b) on ITO-coated glass slide in a 0.1 M DCM/ACN/TBAPF ₆ solvent–electrolyte couple.	48

Figure 3.11 Scan rate dependence of PTQT (a) and PEQT (b) film for p- doping in 0.1 M ACN/TBAPF ₆ solvent–electrolyte couple at 100, 200, 300, and 400 mV/s...	49
Figure 3.12 p- and n-type doping of PTQT (a) and PEQT (b) in 0.1 M ACN/TBAPF ₆ .	50
Figure 3.13 Chemical structures and colors of PTQT and PEQT at different potentials.	52
Figure 3.14 Electronic absorption spectra of monomers TQT, EQT, and EQE in DCM and polymers PTQT, PEQT, and PEQE in thin film form.	53
Figure 3.15 Electronic absorption spectra of PTQT (a) and PEQT (b) in 0.1 M ACN/TBAPF ₆ system upon p-type doping.	54
Figure 3.16 Optical transmittance changes of PTQT at 590, 830, and 1500 nm (a) and PEQT at 690, 905, and 1800 nm (b) in 0.1M ACN/TBAPF ₆ system while switching the potentials between their neutral and oxidized states.	55
Figure A.1 ¹ H NMR of 4-bromo-7-(2,3-dihydrothieno[3,4-b][1,4]dioxin-5-yl)benzo[c][1,2,5]thiadiazole	60
Figure A.2 ¹³ C NMR of 4-bromo-7-(2,3-dihydrothieno[3,4-b][1,4]dioxin-5-yl)benzo[c][1,2,5]thiadiazole	61
Figure A.3 ¹ H NMR of EBT	62
Figure A.4 ¹³ C NMR of EBT	63
Figure A.5 ¹ H NMR of Compound 1	64
Figure A.6 ¹ H NMR of TQT	65
Figure A.7 ¹³ C NMR of TQT	66
Figure A.8 ¹ H NMR of EQT	67
Figure A.9 ¹³ C NMR of EQT	68
Figure A.10 HRMS of TQT	69
Figure A.11 HRMS of EQT	69
Figure A.12 CV of copolymerization with TBT:EBE; 2:1 monomer feed ratio.	70
Figure A.13 CV of copolymerization with TBT:EBE; 1:1 monomer feed ratio.	71
Figure A.14 CV of copolymerization with TBT:EBE; 1:2 monomer feed ratio.	72

Figure A.15 CV of copolymerization with TBT:EBE; 1:4 monomer feed ratio..... 72
Figure A.16 CV of copolymerization with TBT:EBE; 1:10 monomer feed ratio..... 73

ABBREVIATIONS

ACN	Acetonitrile
CB	Conduction Band
CP	Conducting Polymer
CV	Cyclic Voltammetry
DAD	Donor Acceptor Donor
DCM	Dichloromethane
E_g	Band Gap Energy
Fc	Ferrocene
HOMO	Highest Occupied Molecular Orbital
ITO	Indium Tin Oxide
LUMO	Lowest Unoccupied Molecular Orbital
NMR	Nuclear Magnetic Resonance
OLED	Organic Light Emitting Diode
OPV	Organic Photo Voltaics
PPy	Polypyrrole
PTh	Polythiophene
P3AT	Poly(3-alkylthiophene)
TBAPF₆	Tetrabutylammonium hexafluorophosphate
VB	Valence Band

CHAPTER 1

INTRODUCTION

1.1 Conjugated Polymers

In 1976, Alan MacDiarmid, Hideki Shirakawa and Alan J. Heeger discovered conductivity in π -conjugated polymers and their ability to be doped over a full range from insulator to metal conductivity. This breakthrough discovery had brought them the Nobel Prize in 2000 as “*for the discovery and development of conductive polymers*”. Also, this new prodigious research area had created a connection between chemistry and condensed-matter physics with different aspects [1].

In general, the conductive ability of π -conjugated polymers generates from linear combinations of p_z orbitals from the carbon atoms in each repeating unit, which is the basis of π -band. In other words, overlapping of π -bonds orthogonal to the backbone of the polymer brings electron delocalization. Hence charge mobility along the backbone can be obtained by this delocalization [2].

The first generation of semiconducting polymers had begun with discovery of conductivity in polyacetylene by Shirakawa et. al. Although, the polyacetylene was known in polymer science as “black powder” for many years, its conductive “silvery thin film” form was found by the miscalculation of the amount of catalyst [1]. This mistake led to emerging of polyacetylene type conducting polymers (first generation). Although many examples in this type of polymers have high conductivity in doped state, industrial usage of them could not be possible owing to their insolubility and non-processability [3].

The challenges in the first generation brought the phenomena focusing on the second generation in semiconducting polymers; solubility (even if in water), processibility

and also multi-purpose use. Polythiophenes and poly(alkylthiophenes) by Heeger et al, [4] polyaniline by Letheby et al [5], and PEDOT by Reynolds et al [6] are some well-presented examples as the second generation and their excellent properties made them to be used for different purposes as sensors [7], active materials for OPVs [8], OLEDs [9], OFETs [10] and ECDs [11].

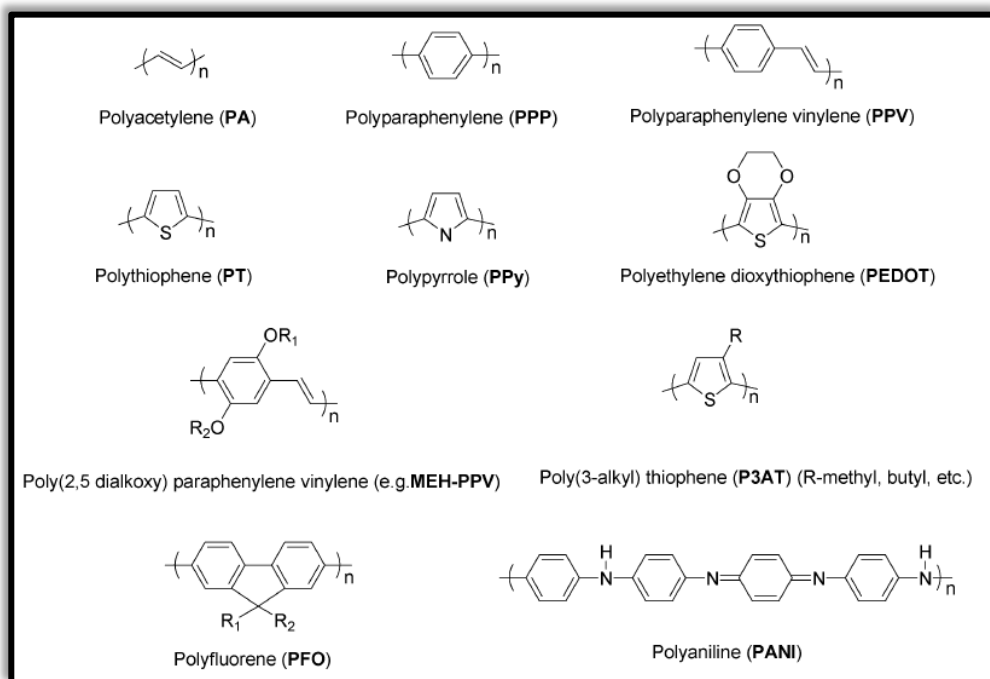


Figure 1.1 Some examples of first and second generation conducting polymers

The enormous attentions on solar energy lead to scientists enhance efficiency of organic solar cells owing to non-improved efficiency of silicone based solar cells. Hence in the past decades, with more complex molecular structures and more

heteroatom in repeating units conducting homo- and co- polymers have synthesized, which is the basis of the third generation conducting polymers [12].

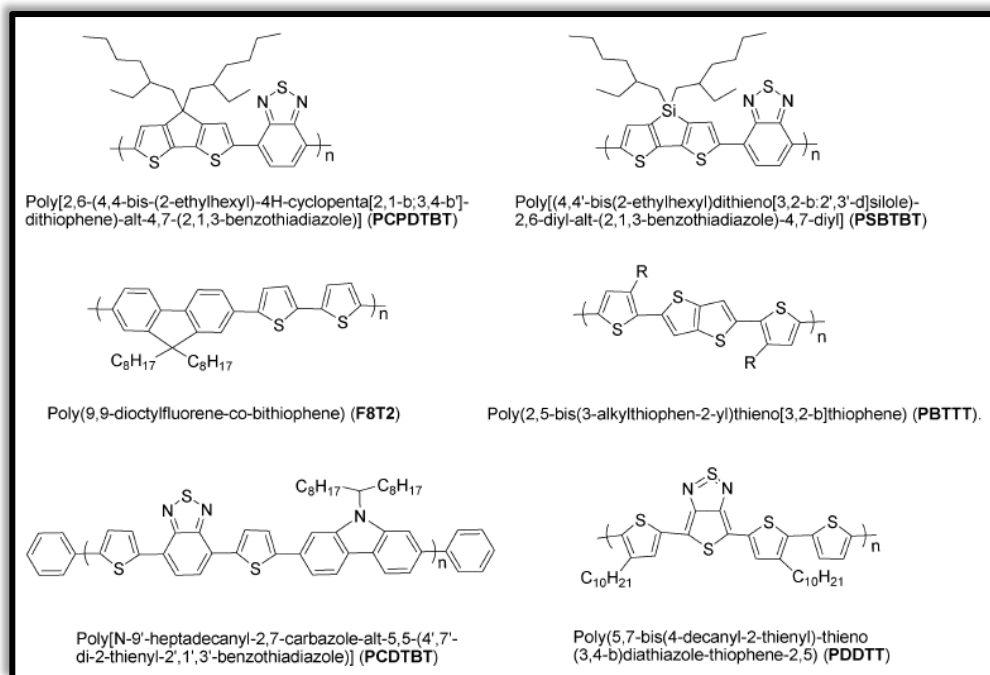


Figure 1.2 Molecular structures of some of the third generation conducting homo- and co- polymers.

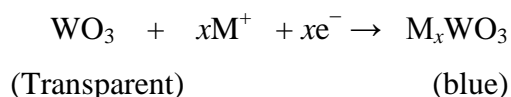
1.2 Electrochromism

Electrochromism can be defined as the non-permanent change in optical properties of a material upon applied potentials. In other words, a material can be defined as electrochromic when it shows remarkable color change in visible region. On the other hand, the definition has been extended by changing optical properties not only

in visible region also in the near infrared [13], thermal infrared and microwave [14] regions.

In 1968, Deb et al. [15] revealed the first example of electrochromic materials and devices. Then, focus on different types of electrochromic materials started due to their high potentials in commercial applications; as display devices [11], mirrors [16] and smart windows [17].

Electrochromic materials could be basically classified in three categories such as metal oxides, molecular dyes and conducting polymers. The most widely known example of metal oxides is the tungsten trioxide (WO_3). During alternation of its optical properties, it is commonly known that the injection/ejection of electrons and metal cations (such as Li^+ , H^+ , etc.) have a noteworthy function on the electrochromic property. Transparent colored (bleached) thin film of WO_3 can be reversed to blue color by the electrochemical reduction as follows:



where; $\text{M}^+ = \text{H}^+$, Li^+ , Na^+ , or K^+ [18].

Besides WO_3 , there are many examples on inorganic electrochromic materials i.e. Prussian Blue systems, oxides of V, Mo, Nb, Ti, Ni, Co, and Ir [19].

Organic small molecular dyes (viologens) are the other example of electrochromic materials. In these molecular dye systems, three redox states are obtained and in the dicationic state (most stable one) the materials reveal no color (bleached). Reduction from this state creates intensely colored radical cations due to optical charge transfer between the oxidized and neutral valent nitrogen atoms [20].

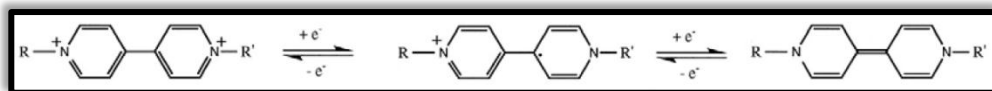


Figure 1.3 Molecular structures of viologens and their different redox states.

1.2.1 Electrochromism in Conducting Polymers

Conductive polymers are one of the most promising electrochromic materials owing to their ease of processibility, (easily synthesis by simple chemical or electrochemical methods and thin film forms could be obtained by easy techniques such as spray coating, spin coating, etc) [21], low cost production, high coloration efficiency [22], independent of angle of vision. In addition, absorption maxima of the polymers could be adjusted by alternation of the electronic character of the π conjugation system from the UV region to the visible and into the near-infrared regions [23]. From these points of view, conductive polymers have gained great attention in common applications of EC materials.

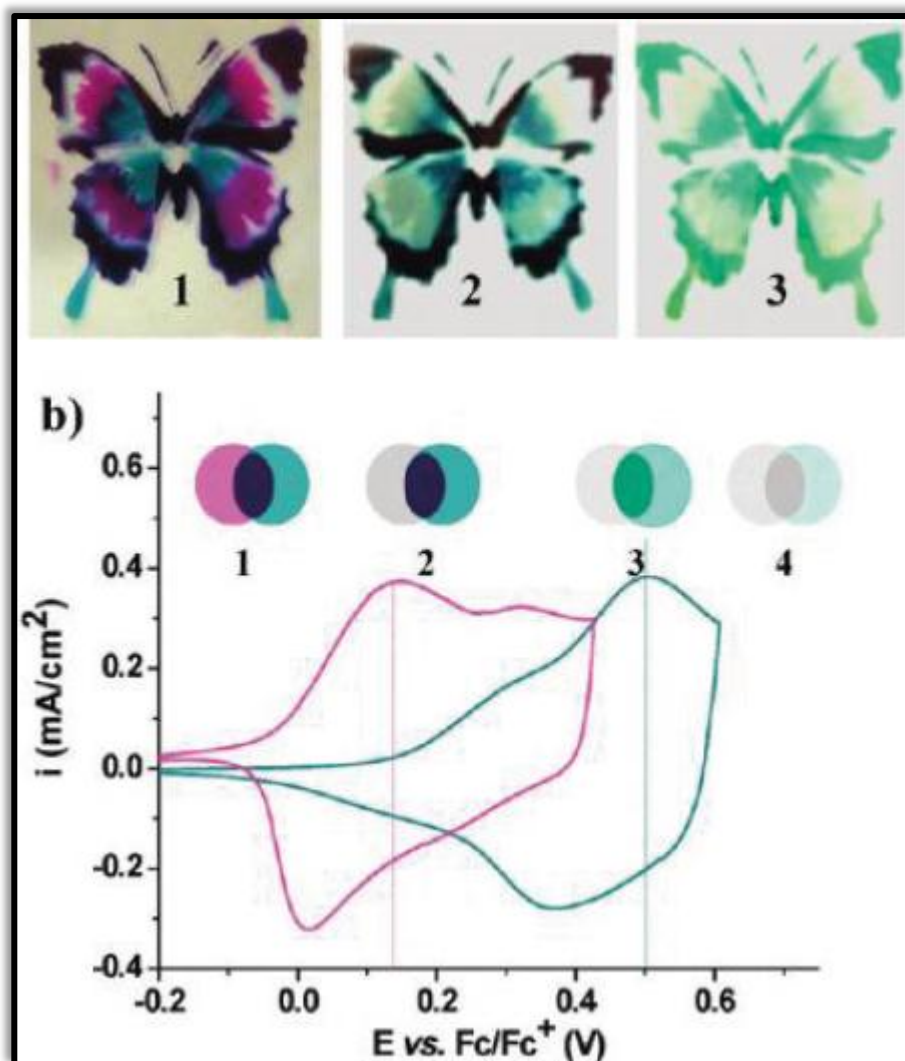


Figure 1.4 One of the examples on electrochromic display device application of conducting polymers

The working principle of electrochromic devices depends on electron injection/ejection to/from the conjugated polymers in active layer of the devices. All the polymers used as an active layer in the devices have semiconducting behavior with a band gap (E_g) in their neutral states. In most of the cases, this energy gap

between their valence and conduction bands leads to an absorption (some cases two simultaneous absorption) at the visible region of spectrum in their neutral state. During the doping processes, some defects (p- or n- type doping) on π -bands along the polymer chain occurred; hence the electronic properties of them become different than the previous state. Moreover, such an electronic change on the polymer causes optical changes, hence the polymer commences to absorb at a different wavelength [24]. For that reasons, PPy, PTh, P3AT, PANI, and PEH-PPV are mostly studied as active materials in electrochromic display devices.

1.3 Band Gap Theory

Band gap theory is used to characterize materials according to their electric conductance ability as insulators, conductors or semiconductors. In conductors, partially filled bands lead to freely motion of charge carriers, hence electrons become mobile. Situation for insulators is opposite to the insulators; fully filled orbitals are not enabling the movement of charge carriers, as a result a drastic gap between valence and conduction band occurs [2]. In a semiconductor, an energy gap (band gap – E_g), less than the one for the insulator separates filled valence and empty conduction bands. Electrons in valence band can transfer to conduction band by either electrochemically or photochemically to generate free charge carriers; holes (p-type) or electrons (n-type) [25].

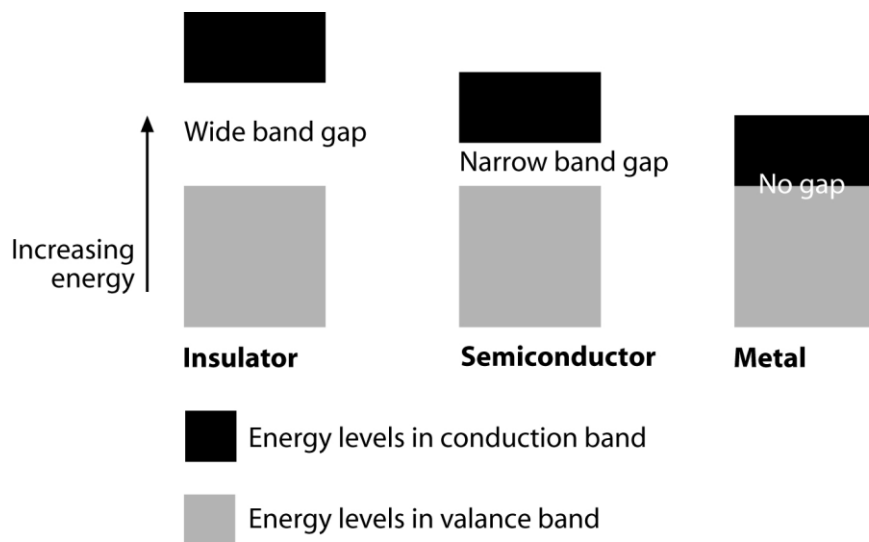


Figure 1.5 Energy level differences of insulator, semiconductor and metal.

The π -conjugated polymers had been known as insulators until Shirakawa et. al. found its conductive form, hence π -conjugated polymers became known as conducting polymers. In their electronic structure, their highest occupied molecular orbital (HOMO, also known as valence band) and their lowest unoccupied molecular orbital (LUMO, also known as conduction band) are separated from each other by a band gap energy. As all semiconductors, conducting polymers could not conduct electricity in their neutral state; on the other hand, after doping process (p- or n-type) generation of free charge carriers lead the movement of electrons and holes easily, hence they become a conductor. For instance, the conductance of the first known conducting polymer could be increased over 15 orders of magnitude by chemically or electrochemically doping, a clear evidence of the presence of band gap in conducting polymers [1].

1.3.1 Factors Affecting the Band Gap

Commercial applications of electrochromic polymers in electronic and photonic devices which bring about controlling the electronic properties (especially band gap) of the polymers is a substantial factor due to the fact that properties of the devices depend on the electronic properties of the neutral semiconducting form of the polymers. For this reason, band gap engineering in electrochromic polymers is a real concern of many scientists.

According to Roncali [26], band gap of a conducting polymer is related to energies of the bond length alternation (E_{BLA}), the mean deviation from planarity (E_{θ}), the inductive and mesomeric electronic effects of substituents (E_{Sub}), the aromatic resonance energy (E_{Res}) and interchain interactions (E_{Int}), hence the band gap could be expressed by the sum of these five contributions as;

$$E_g = E_{BLA} + E_{Res} + E_{Sub} + E_{\theta} + E_{Int}$$

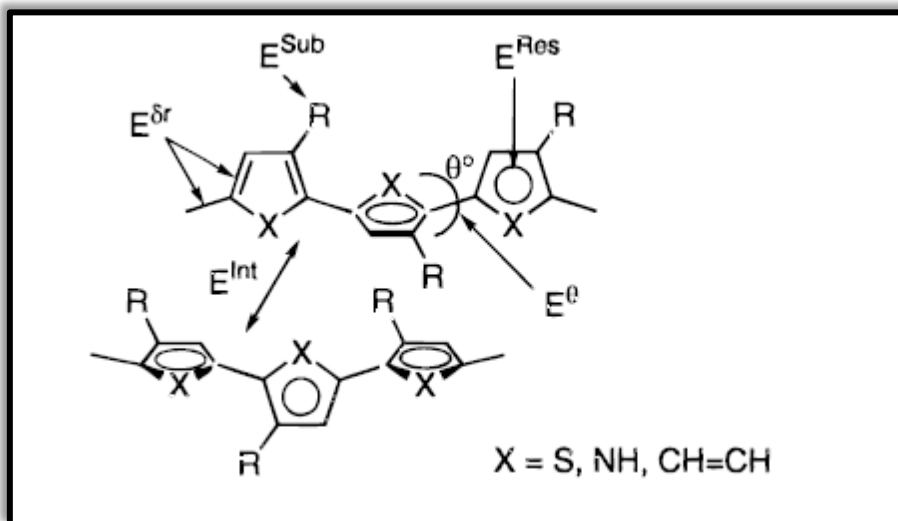


Figure 1.6 Schematic representation of factors affecting E_g

The studies carried out by Bredas [27] define the bond length alternation as “*the maximum difference between the length of a C-C bond that has been inclined relative to the chain axis and a C-C bond that is parallel to the axis.*” Theoretical and experimental studies revealed that one-dimensional conjugated systems are unstable owing to the effects of electron-phonon coupling and electron-electron correlation. As a result, bond length alternation (BLA) makes a major contribution as E_{BLA} to the magnitude of the band gap.

The E_g of conducting polymers are generally proportional to the resonance energy per electron which is related to aromaticity of the polymers. Polyaromatic polymers reveal different electronic structure than polyacetylene due to the fact that their energetically non-equivalent mesomeric forms; aromatic and quinoid, provide both π -electron confinement into the rings and delocalization along the chain. In most examples, quinoid form of the polymers showed smaller band gap. In addition, by inserting polyaromatic groups into the polymer chain quinoid character of the system can be effectively enhanced to reduce the band gap. Polyisothianaphthene (PITN) [28] and poly(dihexylthieno[3,4b]pyrazine) [29] are well-known examples on reduction of E_g by increasing quinoid character. Besides the quinoid character, studies on contribution of heteroatoms in π -conjugated systems to band gap of polymers indicate that lone pairs (or p-orbital) of heteroatoms incorporate with the π -band of the polymers. As a result it affects the aromatic resonance energy (E_{Res}) of the system. The only drawback of fused systems is the lack of stability.

Single bonds between the aromatic cycles in the polymer chain create interannular rotation, leading to corruption of coplanarity in the system [30]. Since π -orbital overlapping changes with the twist angle of two aromatic rings, E_g of polymers can be increased by departure from coplanarity. Up to now, many studies have been done especially on polythiophenes and poly3-alkylthiophenes (P3AT). The results indicated that insertion of flexible side chains to 3-position of thiophene brought steric interactions, in which the rotational distortions rose. Regioregular P3ATs have revealed to have much lower E_g owing to less rotational disorder and more planarity

in the polymer films [31]. Hence, synthesis of electrochromic polymers was tended towards to more planar systems.

In order to modify the HOMO and LUMO levels of π -conjugated systems (also controlling E_g) attaching electron-releasing or –withdrawing groups on the polymer backbone is one of the mostly used methods. By inserting an electron-donating or withdrawing unit, increase of HOMO level or decrease of LUMO level can be achieved. Therefore, increasing the valence band energy or decreasing the conduction band energy leads to lower E_g . For that matter, the most known example is poly(3,4alkoxythiophene)s [6]. The alkoxy unit on the thiophene ring leads to not only soluble polythiophene derivatives but also increasing of HOMO level causes low band gap and oxidation potential of the polymer by electron donating ability.

The last important factor affects the band gap is interactions between polymer chains that may lead to their organizations into a condensed phase. Such an intra- or interchain couplings can make a contribution to band gap of the polymers as E_{int} .

1.3.2 Donor-Acceptor Theory

As mentioned earlier, π -conjugated electrochromic polymers have gained tremendous attention owing to their high potential on usage of many applications in which the band gap of the materials has a major role. For this aim, many approaches have been developed to design and synthesize low band gap polymers such as controlling bond-length alternation (Peierls Distortion), constructing highly planar systems, and stimulating order by interchain effects, resonance effects along the polymer backbone and donor-acceptor approach.

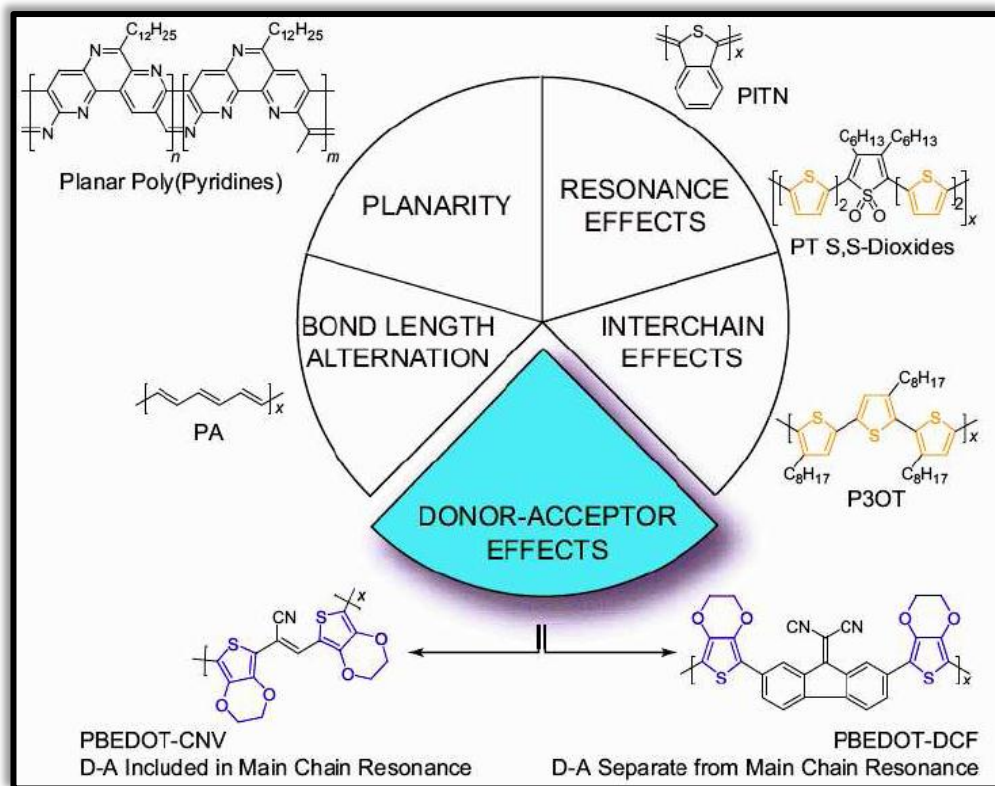


Figure 1.7 Summary of the methodologies using for lowering the band gap

Despite these methods for the synthesis of low band gap polymers are promising, synthesis of donor-acceptor type polymers became superior over the others due to the diversity in synthetic possibility and ease of finding solutions to the solubility problems [32].

Donor-acceptor match leads to a smaller band gap owing to resonances that enable a stronger quinoid character between two units. In addition, hybridization between the energy levels, especially the HOMO of the donor and the LUMO of the acceptor narrows the band gap. As a result, to obtain small band gap polymers, combination of donor units with high HOMO level and acceptor units with low LUMO level leads to smaller band gap than both donor and acceptor unit. Also, donor-acceptor

approach increases third-order nonlinear optical properties of the polymers; hence they can be used in light-emitting diodes, lasers and other applications [33].

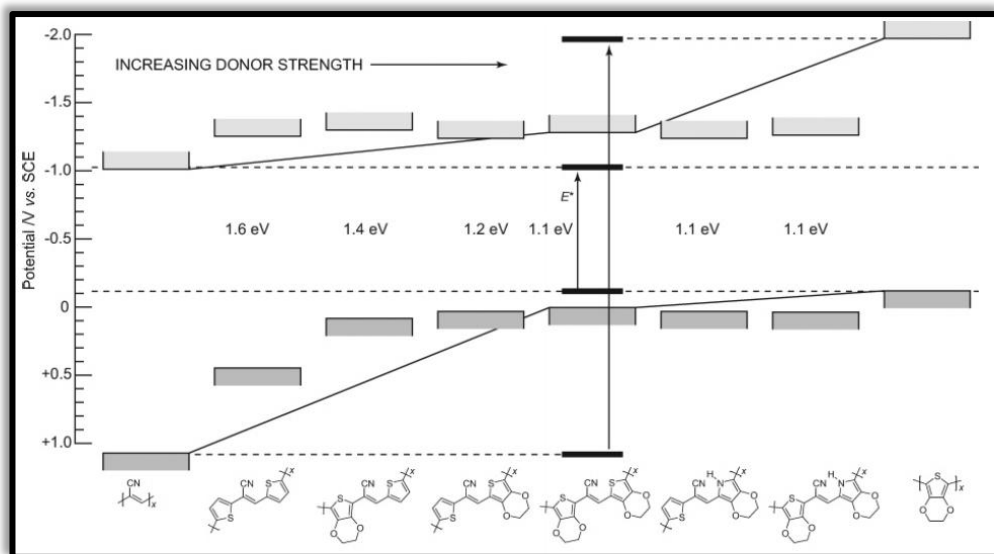


Figure 1.8 Schematic representation of band gap lowering by using different donor units coupling with same acceptor unit.

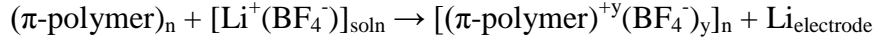
1.4 Electrochemical Doping Process in Conducting Polymers

In order to dope a conducting polymer, chemical, photochemical, interfacial methods can be used [2], however most common method is the electrochemical doping due to being the easiest way to control the doping level [34]. In the electrochemical way, the electrodes inject/eject electrons to the conjugated polymers while counter ions in the electrolyte diffuse into (or out) the polymer chains to

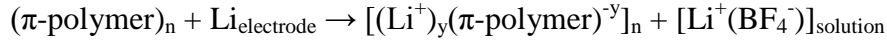
balance electronic charge. Moreover, the doping level of the polymer can be detected by the voltage between the counter electrode and the polymer.

Electrochemical doping can be presented by the following examples:

For p-type:



For n-type:



Structure of conjugated polymers is spoiled from their undoped structure during the doping processes owing to the formation of charge carriers. Moreover, the degree of dopant injected to the polymers is around 10-33 % [35]. Types of charged defects occurred on the polymer backbone, free charge carriers, can be classified as *solitons*, *polarons* and *bipolarons* as seen in Figure 1.8 for polypyrrole. Hence, the energy levels resulted by free charge carriers alters the electronic structure of the polymer, the polymer changes its optical properties according to these new electronic band levels [36].

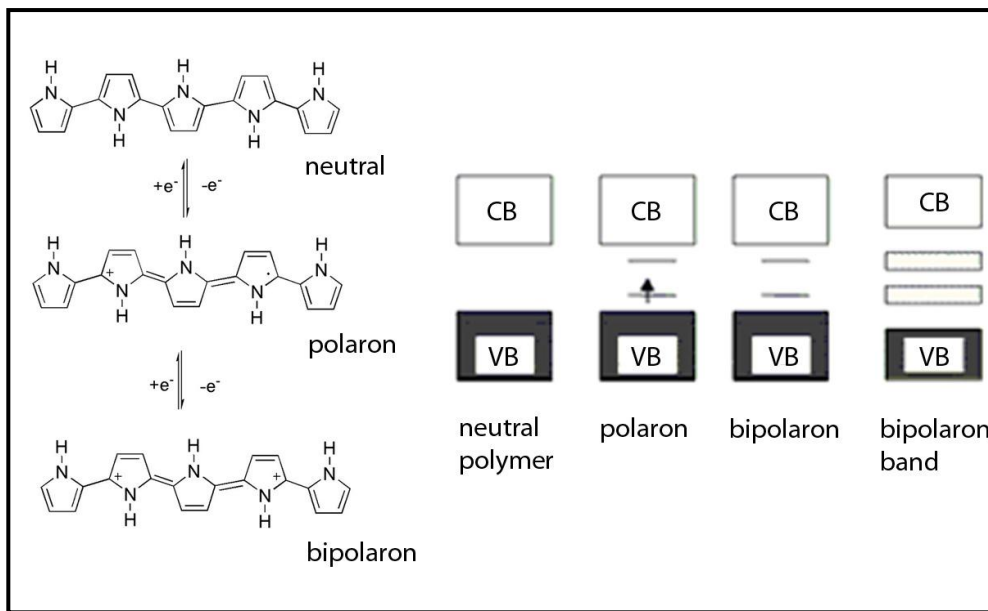


Figure 1.9 Charge carriers in PPy and its corresponding energy bands

1.5 Polymerization Methods

To synthesize conducting polymers, chemical and electrochemical methods are the mostly used techniques due to their ease of applicability. Photochemical polymerization, metathesis polymerization, solid state polymerizations and Grignard reaction are some of other techniques used in producing conducting polymers [37]. Since it is feasible to control the thickness and morphology of polymer film, electrochemical polymerization is a better procedure to synthesize the polymers [38].

1.5.1 Electrochemical Polymerization

Electrochemical synthesis of conducting polymers is a favorable method owing to easy control of the film thickness by the deposition charge.

Mechanism proposed for the electrochemical polymerization of heterocycles begins with the oxidation of the monomer to its radical cation. Coupling of two monomer compounds ensues the first step. The coupling of two monomer compounds can process by two different ways; the combination of two radical cations or addition of radical cation to heterocyclic monomer. After the radical-radical coupling, generated dihydro dimer dication is compelled to release two protons and undergo re-aromatization. Due to the applied potential, the re-aromatized dimer oxidizes to its radical form and gives a further coupling with a monomeric radical. After several steps of re-aromatization and coupling reaction with monomeric radicals, electrochemically synthesized polymer chain is produced [39].

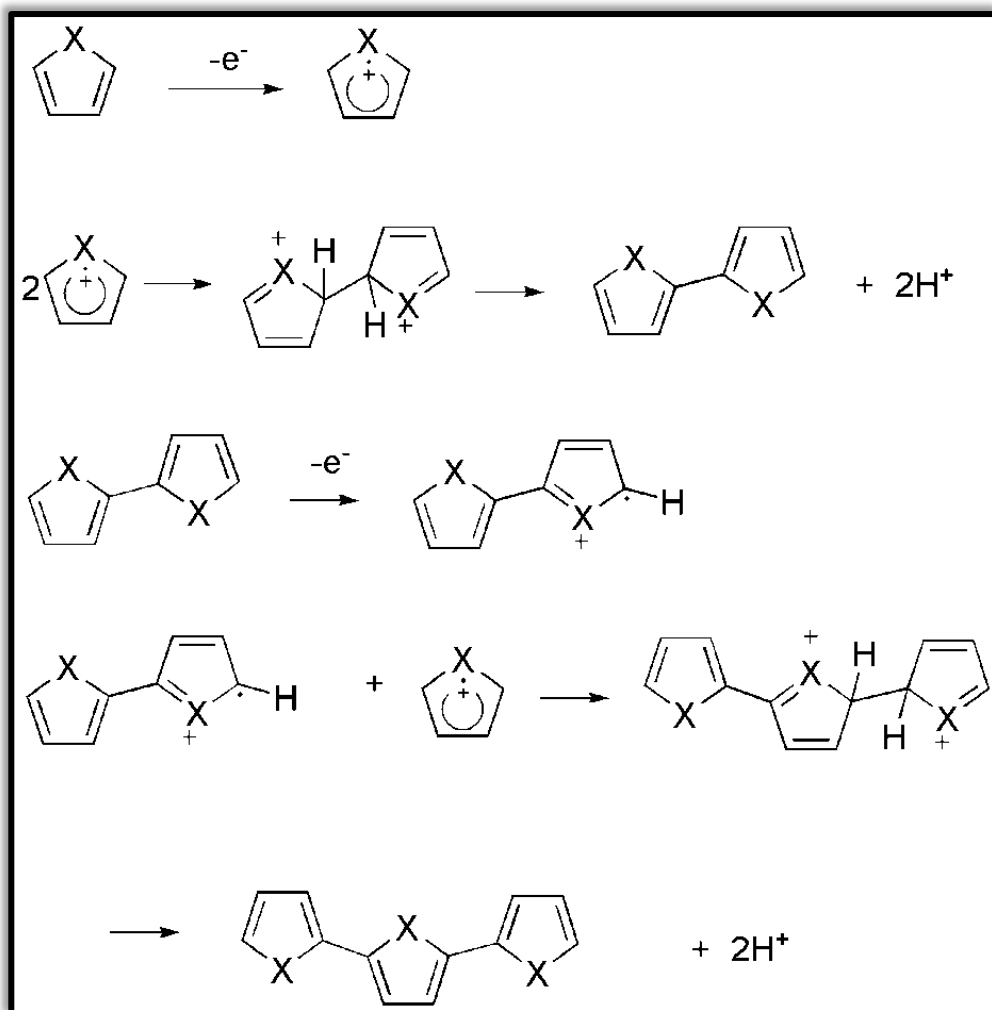


Figure 1.1 Schematic representation of electropolymerization mechanisms of heterocycles (X = S, O, NH)

The only handicap of the technique is that small amounts of polymer which are generally insoluble are produced. As a result, investigation of these polymers with well-known methods like NMR and GPC are not possible.

1.6 Characterization of Electrochromic Polymers

1.6.1 Cyclic Voltammetry (CV)

Cyclic voltammetry is the most widely employed technique to obtain qualitative information concerning electrochemical polymerization. P- or n- type doping potentials and their corresponding dedoping potentials of electroactive compounds can be specified easily by this technique. In this technique the normal three electrode (working, counter and reference electrodes) configuration is used and a potential is applied to the working and counter electrodes sweeping between two values (Figure 1.11) at a fixed rate [40].

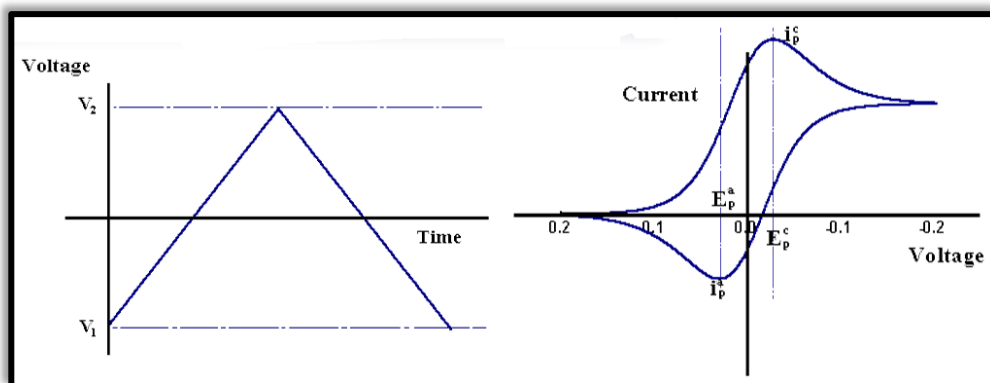


Figure 1.11 Cyclic voltammetry waveform and cyclic voltammogram for a reversible redox reaction.

Also, the resulting current values stemming from the applied potential is recorded by a computer, which indicates the estimated response of a reversible redox peak couple in a single scan (Figure 1.11). The observed peaks in the voltammograms reveal the change in the concentration with time. The peak current for a reversible redox couple can be estimated according to Randles & Sevcik equation [41] as;

$$i_p = 0.4463 n F A C (n F v D / R T)^{1/2}$$

where; i_p : peak height, n : the number of electrons inject/eject in half-reaction for the redox couple, F : Faraday's constant (96485 C/mol), A : electrode area (cm^2), C : the concentration, D : analyte's diffusion coefficient (cm^2/sec), R : universal gas constant (8.314 J / mol K) and T : the absolute temperature (K). At room temperature (25°C/298.15 K) the Randles-Sevcik equation could be written in a more brief way as;

$$i_p = (2.687 \times 10^5) n^{3/2} v^{1/2} D^{1/2} A C$$

Cyclic Voltammetry studies of polymers are performed in a monomer free, electrolyte/solvent couple system.

1.6.2 Spectroelectrochemistry

Spectroelectrochemistry is a concurrent association of electrochemistry and spectroscopy techniques. In order to prove the color and color changes in a scientific method during the doping process, spectroelectrochemistry is the best alternative. Utilization of this technique enables to obtain information about the λ_{max} , band gap, intergap states (polarons and bipolarons) and colors of the polymer.

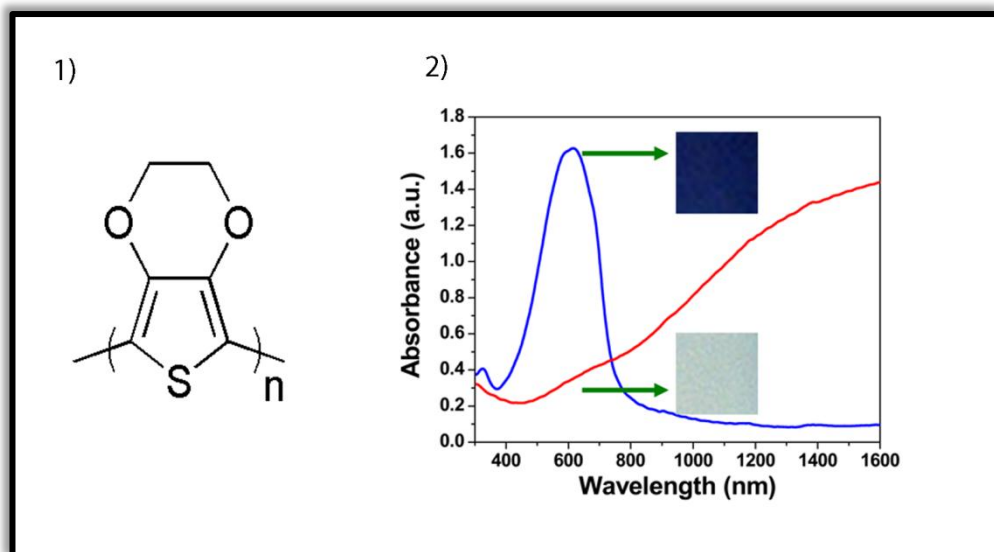


Figure 1.12 1) Structure of mostly used electrochromic polymer; PEDOT and 2) colors of PEDOT in its reduced and oxidized state with its spectra.

During this method, polymer coated ITO as a thin film form is placed into a UV-Vis cuvette which contains electrolyte/solvent couple. As the applied potential increases and the oxidation of polymer stepwise occurs, the alternation of absorption spectrum is monitored by UV-vis-NIR spectroscopy.

1.6.3 Kinetic Studies

Low switching time with high optical contrast in visible or NIR regions and high stability are considered something necessary for electrochromic applications of conducting polymers i.e. electrochromic displays or smart windows. Kinetic studies provide characterization of these features of the polymers. The switching time and contrast (percent transmittance change) can be monitored via square wave potential step method coupled with spectrometry method. With short period of times, the

polymer is oxidized and reduced consecutively, and its optical change at a certain wavelength is recorded as the percent transmittance.

1.7 Aim of This Study

The aims of this study are the investigation of the synthesis of donor-acceptor-donor type monomers by combining two different donor units and electrochemically polymerizing the monomer in order to compare them with the polymers containing one donor unit. For this purpose, two well-known acceptor units; benzo[c][1,2,5]thiadiazole and 2,3-bis(4-(tert-butyl)phenyl)quinoxaline were coupled with 3,4-ethylenedioxythiophene and thiophene units via Stille coupling reaction. The resulted monomers were electrochemically polymerized and their electronic and optical characterizations were achieved. Also, copolymerization of previously synthesized monomers, namely 4,7-di(thiophen-2-yl)benzo[c][1,2,5]thiadiazole (TBT) [42] and 4,7-bis(2,3-dihydrothieno[3,4-b][1,4]dioxin-5-yl)benzo[c][1,2,5]thiadiazole (EBE) [43] with different monomer feed ratios were performed to compare the electronic and optical properties of homo- and co-polymers.

CHAPTER 2

EXPERIMENTAL

2.1 Materials

5,8-Dibromo-2,3-bis(4-tert-butylphenyl)quinoxaline [44], 4,7-dibromobenzo[c][1,2,5]thiadiazole[42-43], tributyl(thiophen-2-yl)stannane[45] and tributyl(2,3-dihydrothieno[3,4-b][1,4]dioxin-5-yl)stannane[46] moieties were synthesized as given in the literature. 4,7-Di(thiophen-2-yl)benzo[c][1,2,5]thiadiazole[42] (TBT) and 4,7-bis(2,3-dihydrothieno[3,4-b][1,4]dioxin-5-yl)benzo[c][1,2,5]thiadiazole[43] (EBE) were synthesized for comparison and performing copolymerization studies and 2,3-bis(4-(tert-butyl)phenyl)-5,8-bis(2,3-dihydrothieno[3,4-b][1,4]dioxin-5-yl)quinoxaline[44] (EQE) was synthesized for comparison purposes. Tributylstanane containing donor units were combined with brominated acceptor units via Stille coupling. For the synthesis of the donor acceptor donor type monomers; 2,1,3-Benzothiadiazole (Aldrich), bromine (Br₂) (Merck), hydrobromic acid (HBr, 47%) (Merck), 3,4-ethylenedioxythiophene (EDOT) (Aldrich), sodium borohydride (NaBH₄) (Merck), thiophene (Th) (Aldrich), 4-tert-butylbenzaldehyde (Aldrich), p-toluenesulfonic acid (PTSA) (Aldrich), ethanol (EtOH) (Aldrich), potassium cyanide (KCN) (Aldrich), hexane (C₆H₁₄) (Merck), chloroform (CHCl₃) (Aldrich), dichloromethane (CH₂Cl₂) (Aldrich), n-butyllithium (n-BuLi, 2.5M in hexane) (Acros Organics), tributyltin chloride (Sn(Bu)₃Cl, 96%) (Aldrich), diethylether (Et₂O) (Merck), bis(triphenylphosphine)palladium(II) dichloride (Aldrich) were used as received.

Tetrahydrofuran (THF) (Fisher) was used by drying over benzophenone (Merck) and sodium.

2.2 Equipments

^1H - NMR and ^{13}C -NMR spectra were recorded in CDCl_3 on a Bruker Spectrospin Avance DPX-400 Spectrometer. Chemical shifts were given in ppm downfield from tetramethylsilane. Products were purified via column chromatography with Merck Silica Gel 60 (particle size: 0.040–0.063 mm, 230–400 mesh ASTM). HRMS studies were done with a Waters SYNAPT MS system. Electrochemical studies were performed in a three-electrode cell consisting of an Indium Tin Oxide (ITO) coated glass slide as the working electrode, platinum (Pt) wire as the counter electrode, and silver (Ag) wire as the pseudo reference electrode under ambient conditions using Voltalab PST050 and Solartron 1285 potentiostats. Before each measurement, solutions were purged with nitrogen for 5 min. For the calculation of HOMO and LUMO level of the polymers, the value of Standard Hydrogen Electrode (SHE) was taken as -4.75 eV [47]. After each measurement, the reference electrode was calibrated against Fc/Fc^+ . Solvents were spectrophotometric grade. Varian Cary 5000 UV–Vis spectrophotometer was used to perform the spectroelectrochemical studies of the polymer.

2.3 Synthesis of Monomers

2.3.1 Synthesis of 4-bromo-7-(2,3-dihydrothieno[3,4-b][1,4]dioxin-5-yl)benzo[c][1,2,5]thiadiazole

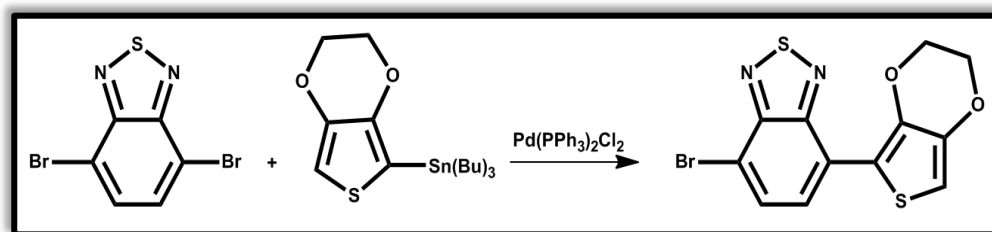


Figure 2.1 Synthetic route for 4-bromo-7-(2,3-dihydrothieno[3,4-b][1,4]dioxin-5-yl)benzo[c][1,2,5]thiadiazole

4,7-Dibromobenzo[c][1,2,5]thiadiazole (1.5 g, 5.1 mmol) and tributyl(2,3-dihydrothieno[3,4-b][1,4]dioxin-5-yl)stannane (3.3 g, 7.7 mmol) were dissolved in dry tetrahydrofuran (THF) (60 ml) and set for refluxing under argon atmosphere. The catalyst, dichlorobis(triphenylphosphine)-palladium(II) (60 mg, 0.085x10⁻³ mmol) was added and the mixture was stirred at 100 °C under argon atmosphere for 16h while monitoring the reaction with TLC. At the end of 16 h, the mixture was cooled and THF was removed from the mixture by rotary evaporator. Then the residue was subjected to column chromatography (chloroform: hexane, 3:1) to

afford a purple solid, 4-bromo-7-(2,3-dihydrothieno[3,4-b][1,4]dioxin-5-yl)benzo[c][1,2,5]thiadiazole. ^1H NMR (400 MHz, CDCl_3): δ (ppm) 7.77 (d, 1H), 8.16 (d, 1H), 6.54 (s, 1H), 4.24 (m, 2H), 4.34 (m, 2H). ^{13}C NMR (100 MHz, CDCl_3): δ (ppm) 61.95, 62.73, 100.63, 105.36, 115.65, 123.47, 124.02, 127.67, 127.84, 130.21, 139.34, 151.15.

2.3.2 Synthesis of 4-(2,3-dihydrothieno[3,4-b][1,4]dioxin-5-yl)-7-(thiophen-2-yl)benzo[c][1,2,5]thiadiazole (EBT)

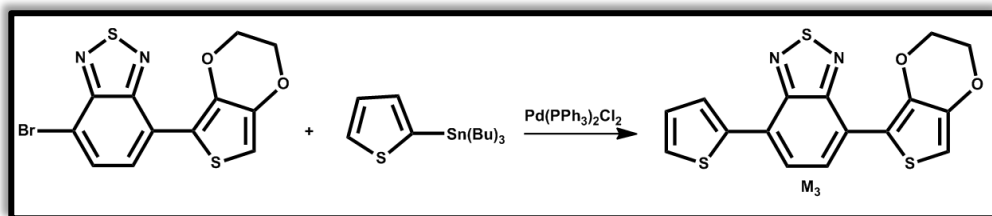


Figure 2.2 Synthetic route for 4-(2,3-dihydrothieno[3,4-b][1,4]dioxin-5-yl)-7-(thiophen-2-yl)benzo[c][1,2,5]thiadiazole (EBT)

4-Bromo-7-(2,3-dihydrothieno[3,4-b][1,4]dioxin-5-yl) benzo[c][1,2,5]thiadiazole (1 g, 2.8 mmol), and tributyl(thiophen-2-yl)stannane (2.1 g, 5.6 mmol) were dissolved in THF (60 ml) and dichlorobis(triphenylphosphine)-palladium(II) (50 mg, 0.071×10^{-3} mmol) was added and the mixture was refluxed at 100 °C under argon atmosphere for 12h. Solvent was evaporated under vacuum and the crude product was purified by column chromatography (chloroform: hexane, 3:1) to obtain a dark red solid, 4-(2,3-dihydrothieno[3,4-b][1,4]dioxin-5-yl)-7-(thiophen-2-

)benzo[c][1,2,5]thiadiazole (TBE) . ^1H NMR (400 MHz, CDCl_3): δ (ppm) 6.5 (s, 1H), 7.8 (d, 1H), 6.9 (s, 2H), 8.3 (d, 1H), 8.0 (m, 1H), 7.1 (m, 1H), 7.4 (m, 1H), 4.3 (m, 2H), 4.2 (m, 2H); ^{13}C NMR (100 MHz, CDCl_3): δ (ppm) 151.56, 151.38, 140.70, 140.66, 140.37, 139.21, 138.32, 126.64, 125.90, 125.11, 124.92, 124.85, 123.51, 101.13, 63.75, 63.04.

2.3.3 Synthesis of 2,3-Bis(4-tert-butylphenyl)-5,8-di(thiophen-2-yl)quinoxaline (TQT) and 5-Bromo-2,3-bis(4-tert-butylphenyl)-8-(thiophen-2-yl)quinoxaline (1)

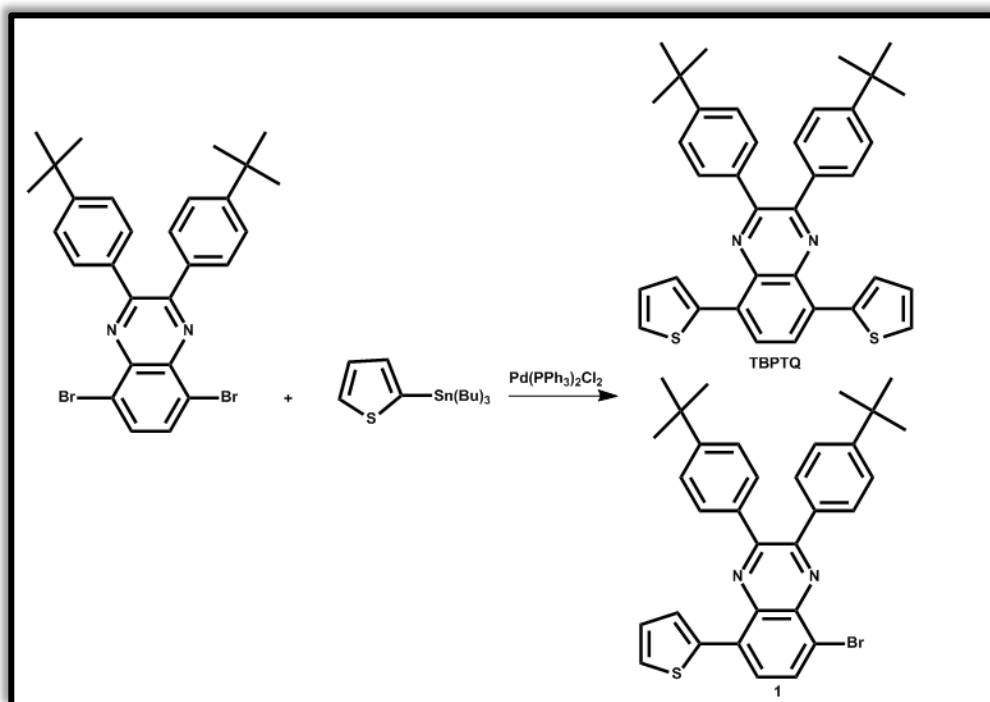


Figure 2.3 Synthetic pathway for 2,3-bis(4-tert-butylphenyl)-5,8-di(thiophen-2-yl)quinoxaline (TQT) and 5-bromo-2,3-bis(4-tert-butylphenyl)-8-(thiophen-2-yl)quinoxaline (1)

5,8-Dibromo-2,3-bis(4-tert-butylphenyl)quinoxaline (1.5 g, 2.72 mmol) and tributyl(thiophen-2-yl)stannane (3.04 g, 8.15 mmol) were dissolved in dry THF (60 mL) and refluxed under argon atmosphere. The catalyst, dichlorobis(triphenylphosphine)-palladium(II) (60 mg, 0.085x10⁻³ mmol), was added, and the mixture was stirred at 100 °C under argon atmosphere for 16 h while monitoring the reaction with TLC. At the end of 16 h, the mixture was cooled and THF was removed from the mixture by rotary evaporator. Then, the residue was subjected to column chromatography (dichloromethane:hexane, 1:1) to afford a yellow-orange solid, 2,3-bis(4-tert-butylphenyl)-5,8-di(thiophen-2-yl)quinoxaline and a yellow solid, 5-bromo-2,3-bis(4-tert-butylphenyl)-8-(thiophen-2-yl)quinoxaline. ¹H NMR (for TQT) (400 MHz, CDCl₃): δ (ppm) 1.27 (s, 18H), 7.08 (m, 2H), 7.31 (d, 4H), 7.42 (d, 2H), 7.63 (d, 4H), 7.76 (d, 2H), 7.99 (s, 2H). ¹³C NMR (for TQT) (100 MHz, CDCl₃): δ (ppm) 31.33, 34.78, 125.15, 126.38, 126.60, 126.81, 128.69, 130.17, 131.19, 135.94, 137.09, 138.94, 151.70, 152.19. HRMS-ESI⁺ (m/z): Calcd (C₃₆H₃₄N₂S₂) 559.2242, found 559.2255.

¹H NMR (for **1**) (400 MHz, CDCl₃): δ (ppm) 1.27 (s, 9H), 1.28 (s, 9H), 7.10 (m, 1H), 7.31 (d, 2H), 7.33 (d, 2H), 7.47 (d, 1H), 7.59 (d, 2H), 7.61 (d, 2H), 7.77 (d, 1H), 7.86 (d, 1H), 7.95 (d, 1H). ¹³C NMR (for **1**) (100 MHz, CDCl₃): δ (ppm) 31.33, 31.89, 34.78, 35.02, 125.15, 125.76, 126.38, 126.95, 126.60, 126.81, 127.02, 127.51, 128.69, 129.03, 130.17, 131.19, 131.82, 135.94, 137.09, 138.94, 151.70, 152.07, 152.19, 153.08.

2.3.4 Synthesis of 2,3-Bis(4-tert-butylphenyl)-5-(2,3-dihydrothieno[3,4-b][1,4]dioxin-5-yl)-8-(thiophen-2-yl)quinoxaline (EQT)

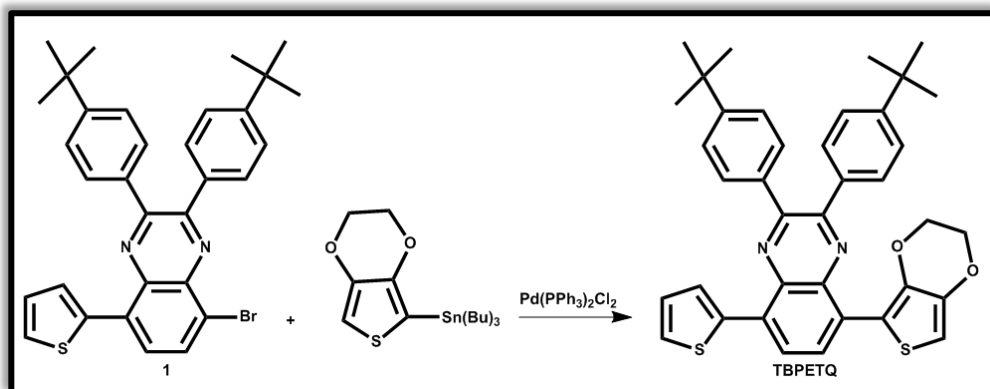


Figure 2.4 Synthetic route for 2,3-Bis(4-tert-butylphenyl)-5-(2,3-dihydrothieno[3,4-b][1,4]dioxin-5-yl)-8-(thiophen-2-yl)quinoxaline EQT

Compound **1** (1.5 g, 2.7 mmol) and tributyl(2,3-dihydrothieno[3,4-b][1,4]dioxin-5-yl)stannane (2.34 g, 5.4 mmol) were dissolved in dry THF (60 mL) and refluxed under argon atmosphere. The catalyst, dichlorobis(triphenylphosphine)-palladium(II) (60 mg, 0.085x10⁻³ mmol), was added, and the mixture was stirred at 100 °C under argon atmosphere for 16 h while monitoring the reaction with TLC. At the end of 16 h, the mixture was cooled and THF was removed from the mixture by rotary evaporator. Then, the residue was subjected to column chromatography

(chloroform:hexane, 2:1) to afford a orange solid, 2,3-bis(4-tert-butylphenyl)-5-(2,3-dihydrothieno[3,4-b][1,4]dioxin-5-yl)-8-(thiophen-2-yl)quinoxaline (EQT).

^1H NMR (400 MHz, CDCl_3): δ (ppm) 1.27 (s, 9H), 1.28 (s, 9H), 4.21 (m, 2H), 4.31 (m, 2H), 6.51 (s, 1H), 7.09 (m, 1H), 7.30 (d, 1H), 7.41 (d, 2H), 7.42 (d, 2H), 7.63 (d, 1H), 7.76 (d, 2H), 7.77 (d, 2H), 8.02 (d, 1H), 8.50 (d, 1H). ^{13}C NMR (100 MHz, CDCl_3): δ (ppm) 31.32, 31.56, 34.77, 34.89, 64.36, 65.02, 103.04, 113.34, 125.11, 126.17, 126.56, 126.95, 127.67, 128.38, 128.41, 129.85, 129.95, 130.16, 130.26, 135.80, 136.01, 136.89, 137.14, 139.17, 140.39, 141.38, 151.05, 151.40, 152.08, 152.12. HRMS-ESI⁺ (m/z): Calcd ($\text{C}_{38}\text{H}_{38}\text{N}_2\text{S}_2\text{O}_2$) 617.2296, found 617.2297.

2.4 Synthesis of the Polymers

2.4.1 Homopolymerization of EBT

The corresponding polymer of EBT; PEBT, was potentiodynamically produced via electrochemical polymerization on an ITO coated glass slide electrode. EBT (10 mM) was polymerized in 0.1 M tetrabutylammonium hexafluorophosphate (TBAPF_6)/ dichloromethane (CH_2Cl_2)/ acetonitrile (ACN) (5: 95, v: v) solution with applied potentials between -0.3 and 1.5 V. After the polymerization, homopolymers were washed with ACN in order to remove the excess supporting electrolyte and unreacted monomer [48].

2.4.2 Copolymerization of TBT and EBE

Copolymer studies were performed with TBT and EBE in order to observe whether the resulting copolymer will have the same properties with PEBT. A three-electrode cell with ITO working electrode was used to deposit copolymers potentiodynamically. Oxidative polymerizations were achieved by repeated cycling between -0.3 V and +1.5 V with different feed ratios. For 1:1 (TBT:EBE) ratio 10^{-6} moles of each comonomer were used and the other ratios were determined according

to the mole ratios. $\text{CH}_2\text{Cl}_2/\text{ACN}$ (5: 95 v: v)/ TBAPF_6 solvent-electrolyte system was used for polymerization at a scan rate of $100 \text{ mV}\cdot\text{s}^{-1}$ for 1:1, 1:2, 1:4, 1:10 and 2:1 (TBT:EBE) ratios. A structural representation of the reaction taking place during electrochemical copolymerization is shown in figure 2.5 [48].

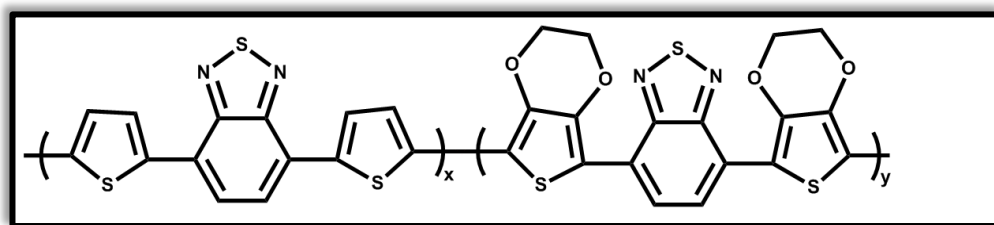


Figure 2.5 Structural representations of electrochemical copolymers

2.4.3 Homopolymerization of TQT and EQT

10 mM of monomer solutions in 0.1 M tetrabutylammonium hexafluorophosphate (TBAPF_6)/ dichloromethane (CH_2Cl_2)/ acetonitrile (ACN) (5: 95, v: v) were placed into electrochemical polymerization cell and TQT and EQT were polymerized potentiodynamically with applied potentials between 0 and 1.4 V and -0.2 and 1.3 V, respectively, versus Ag wire pseudo-reference electrode. After the polymerization, homopolymers were washed with ACN in order to remove the excess supporting electrolyte and unreacted monomer [49].

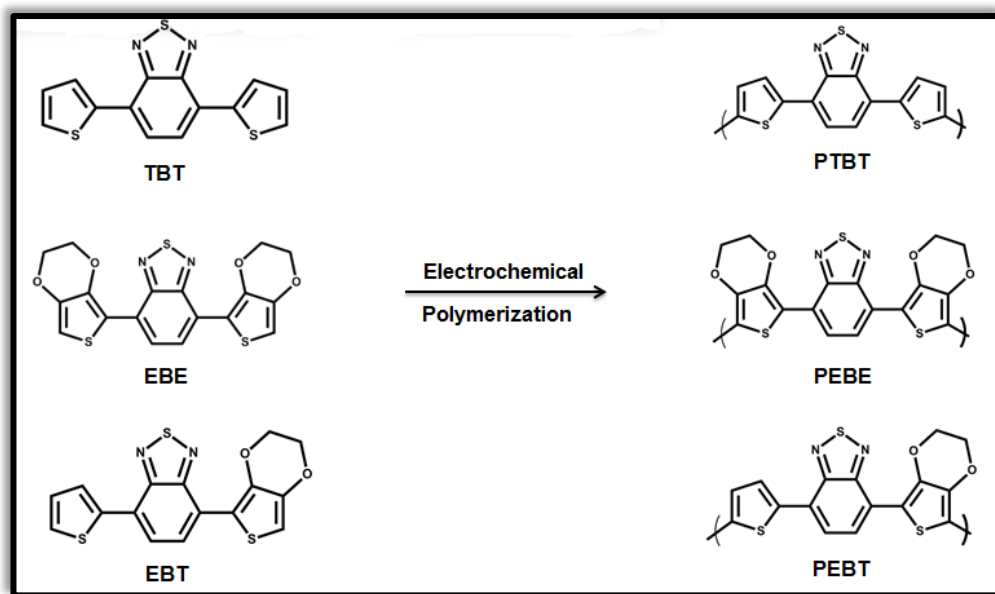


Figure 2.6 Chemical structures of benzothiadiazole bearing monomers and their corresponding polymers

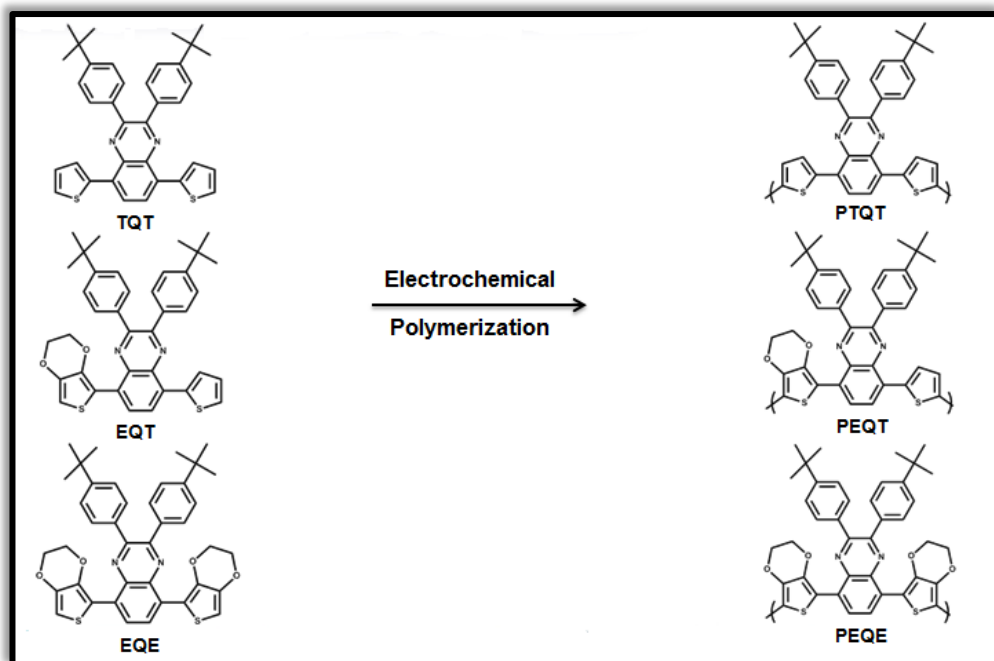


Figure 2.7 Chemical structures of quinoxaline bearing monomers and their corresponding polymers

CHAPTER 3

RESULTS AND DISCUSSION

3.1 Electrochemical and Optical Properties of Benzothiadiazole Derivative Homo- and Co-polymers

3.1.1 Electrochemical and Optical Properties of PEBT

3.1.1.1 Electrochemistry of PEBT

EBT was polymerized potentiodynamically at potentials between -0.3 V and 1.5 V vs. Ag wire pseudo reference electrode in a 0.1 M dichloromethane (DCM)/acetonitrile (ACN) (5:95, v:v)/tetrabutylammonium hexafluorophosphate (TBAPF₆) solution onto indium tin oxide (ITO)-coated glass slides. During polymerization, a characteristic oxidation peak was observed at 1.2 V accompanied by a reversible redox couple for polymer as seen in Figure 3.1. The increase in current density with the number of scans clearly shows the deposition of an electroactive film of PEBT on ITO. The resultant polymer revealed reversible p-type doping properties where p doping and de-doping were indicated by the peaks at 1.06 V and 0.85 V, respectively.

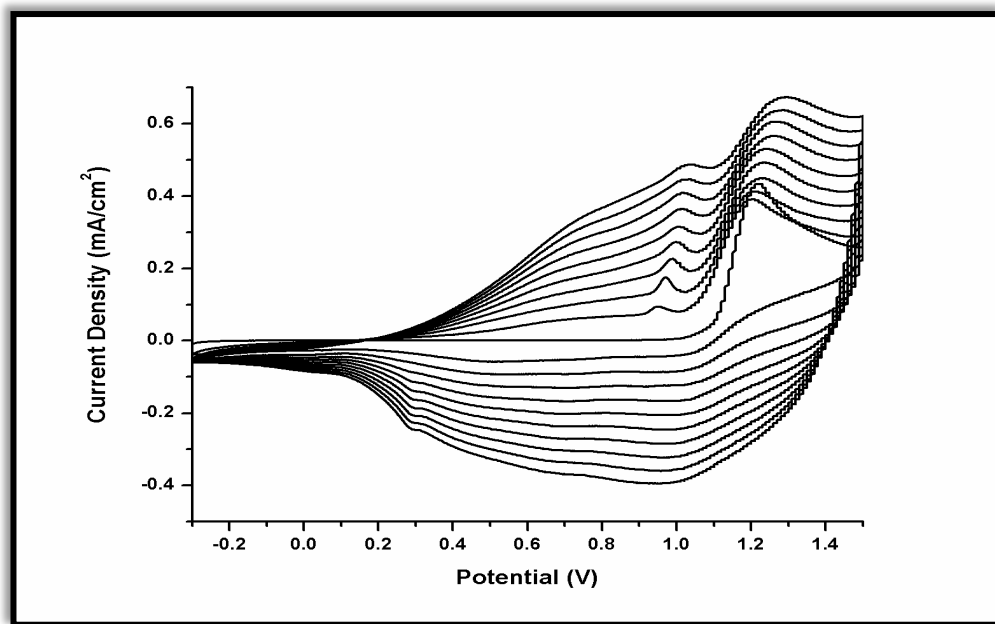


Figure 3.1 Electrochemical deposition of PEBT on ITO-coated glass slide in a 0.1 M DCM/ACN/TBAPF₆ solvent-electrolyte couple

Since the polymer structure consists of electron withdrawing benzothiadiazole units, a rare property; n-type doping was observed for PEBT given with reversible peaks at -1.6 V and -1.0 V vs. the same reference electrode (Figure 3.2). Oxidation and reduction onset values were used to determine the band gap energies for PEBT since the polymer is both p- and n-type dopable. HOMO and LUMO energies were calculated as -5.00 and -3.75 eV, respectively (the value of NHE was used as 4.75 eV throughout this study), and as a result electronic band gap (E_g^{el}) of the polymer was found to be 1.25 eV.

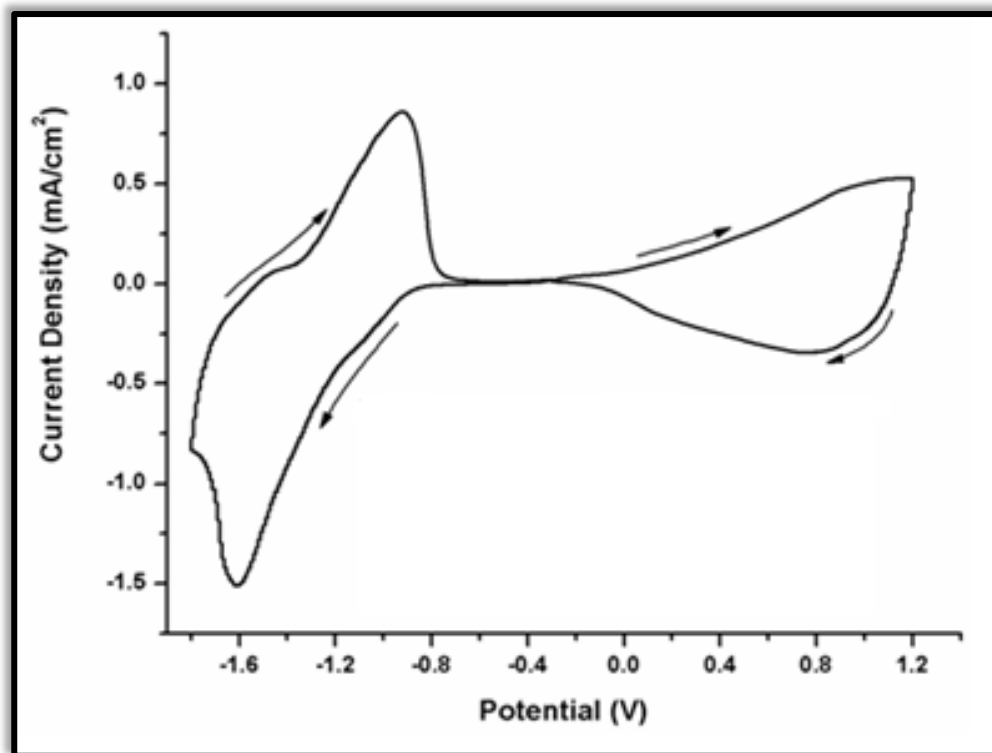


Figure 3.2 p- and n-doping of PEPT

The scan rate dependence of the PEPT film was investigated using CV. A direct proportionality between the scan rate and the current intensity indicates a well adhered electroactive film on ITO and a non-diffusion controlled electrochemical process. As demonstrated in Figure 3.3, the linear relationship can be seen even at very low and high scan rates which demonstrate that the number of electrons in the diffusion layer is always constant during the scans but increases as the scan rate increases.

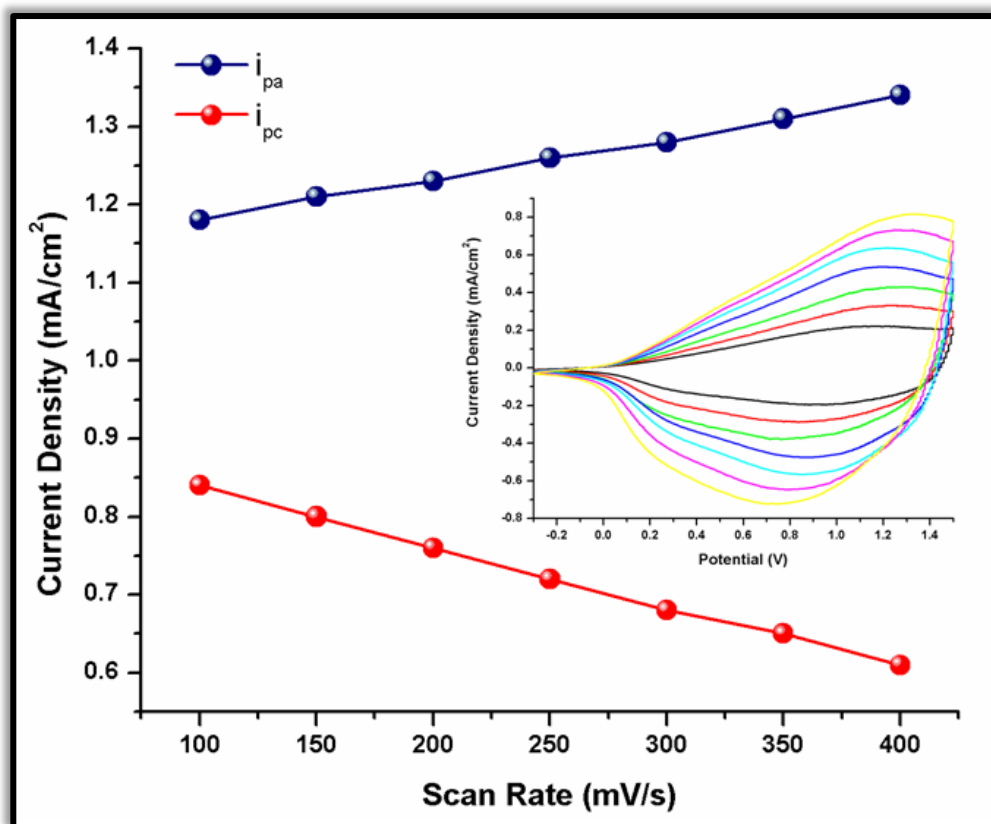


Figure 3.3 Scan rate dependence of PEBT film for p-doping in 0.1 M ACN/TBAPF₆ solvent-electrolyte couple at 100, 150, 200, 250, 300, 350 and 400 mV.s⁻¹.

3.1.1.2 Optical Properties of P₃

To investigate the spectral response of PEBT upon p-doping process, in situ UV-Vis-NIR spectra were monitored in a monomer free 0.1 M ACN/ TBAPF₆ solution under applied potentials. As all donor-acceptor-donor type polymers in the literature, PEBT revealed two absorption maxima; the π - π^* transitions of the conjugated polymers was seen in the short wavelength region at 408 nm, and in the long

wavelength region at 642 nm is owing to the intramolecular charge transfer transitions between the donor and the acceptor units as shown in Figure 3.4. Hence, PEBT has a greenish-blue color in its neutral state. In order to have a green color, there should be two transitions at around 400 nm and 700 nm in the visible region. Although PEBT has two simultaneous absorptions in the visible region, it still does not reveal green color since the second π - π^* transition is not at around 700 nm.

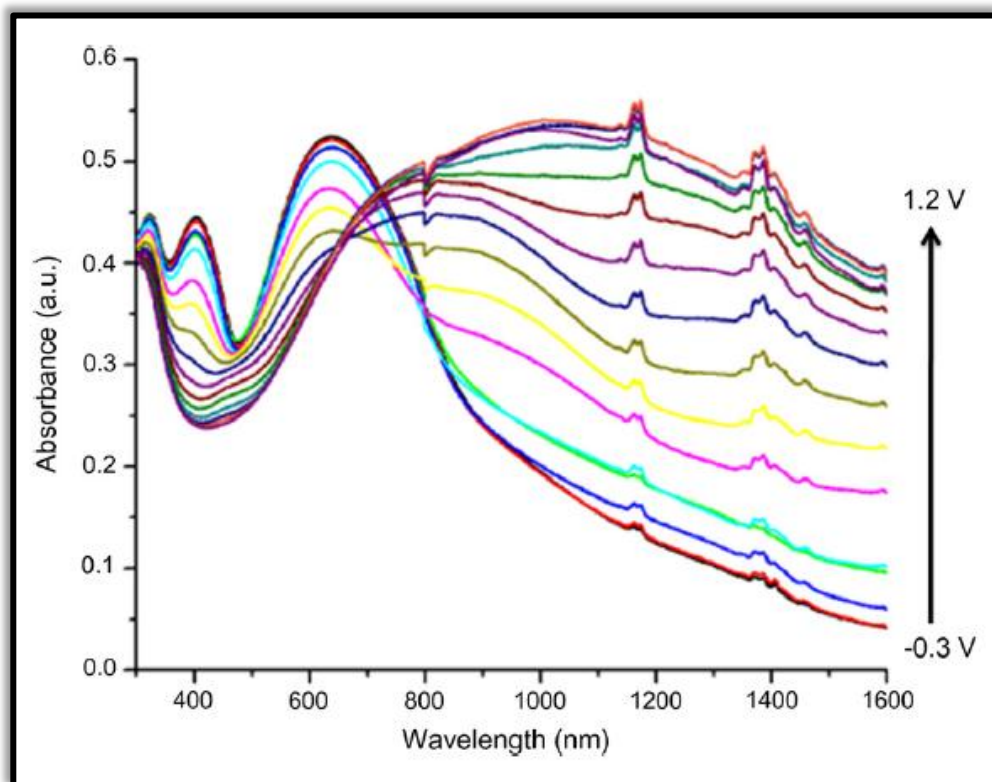


Figure 3.4 Electronic absorption spectra of PEBT in 0.1 M ACN/TBAPF₆ system upon p-type doping process

The optical band gap (E_g^{op}) of PEBT was calculated as 1.18 eV from the onset of the low energy π - π^* transition. During stepwise oxidation, the potential was gradually increased from 0.3 V to 1.2 V and the absorbance changes were observed. In its neutral form PEBT revealed only two transitions with no absorbance in NIR region. Upon p-type doping, as the peaks at 408 nm and 642 nm were depleted, new bands in NIR region intensified due to the charge carrier formation such as polarons and bipolarons (Figure 3.4). Since PEBT still absorbs after 600 nm in its doped state, the polymer was light blue. Also, in order to have a transmissive state in the doped form the bands in the visible region should have depleted completely.

During investigation of electronic properties of PEBT, it revealed reversible n-type redox couple and changed its color. However, to prove such an n-type doping process there should be evidence for considerable optical differences after the introduction of charge carries to the conjugated system. As shown in Figure 3.5, accretion of bands in the NIR absorption region upon n-type doping of PEBT is clear evidence for formation of negative charge carriers. Also, the polymer absorbs nearly entire visible region, dark-gray color was seen in its n-doped state.

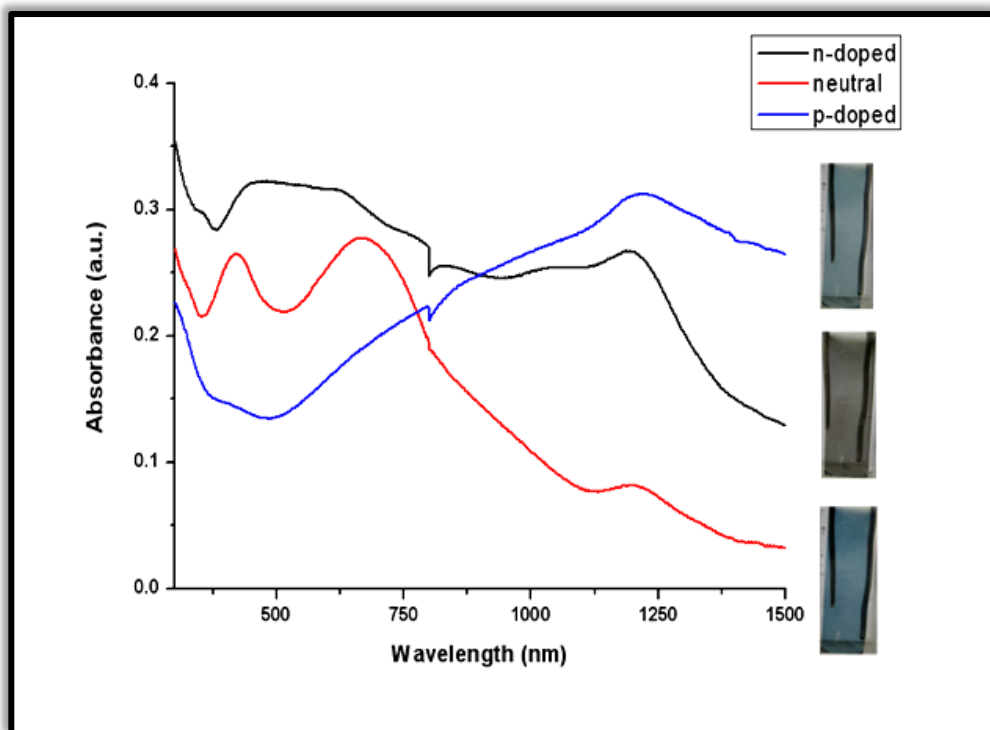


Figure 3.5 Optical changes of P₃ in neutral, p- and n- doped states.

Transmittance changes and switching abilities of PEBT were determined while sweeping the potentials between its fully oxidized and reduced states within 5 s time intervals. The studies were performed in a monomer free 0.1 M ACN/TBAPF₆ solvent-electrolyte system. PEBT revealed 22 % transmittance change upon doping/de-doping process at 408 nm, 14 % at 620 nm and 46 % at 1050 nm (Figure 3.6). Switching time is the duration for the polymer to switch between the two extreme states and it was calculated as 0.6 s, 0.75 s and 0.8 s at corresponding wavelengths.

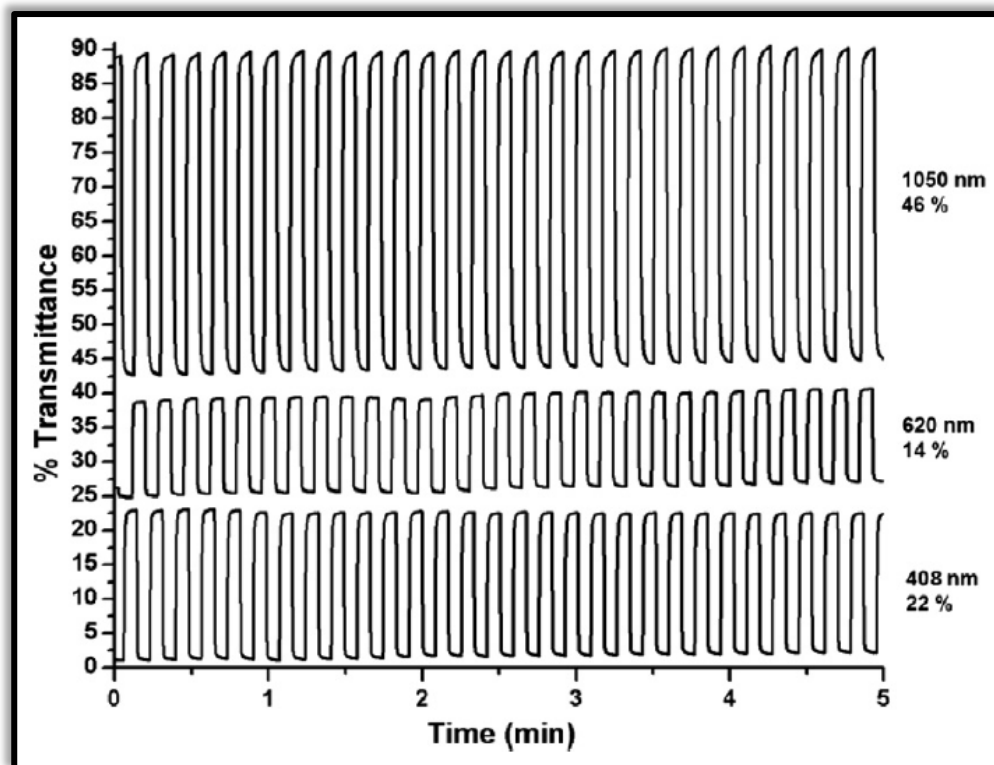


Figure 3.6 Optical transmittance changes of PEBT at 408 nm, 620 nm and 1050 nm in 0.1 M ACN/TBAPF₆ system while switching the potentials between its neutral and oxidized states

3.1.2 Comparison of PEBT with Its Homologous PTBT and PEBE

In literature, electrochemical studies of TBT and EBE were reported in 0.1 M DCM/ACN (5:95, v:v)/TBAClO₄ and DCM/TBAPF₆ vs. the Ag/Ag⁺ reference electrode. In order to have a reliable comparison with M₃, all experiments were performed in DCM/ACN/TBAPF₆ system vs. Ag wire pseudo reference electrode. Generally, EDOT bearing DAD type molecules have lower monomer oxidation potentials than those of thiophene bearing ones under identical

experimental conditions owing to the electron rich ethylenedioxythiophene group. As a result, EBT revealed a monomer oxidation at 1.2 V vs. Ag wire pseudo reference electrode which was lying between the other two. Since EBT contains ethylenedioxythiophene and thiophene groups, its oxidation potential value is between the values of the monomers containing only EDOT or thiophene as shown in Figure 3.7.

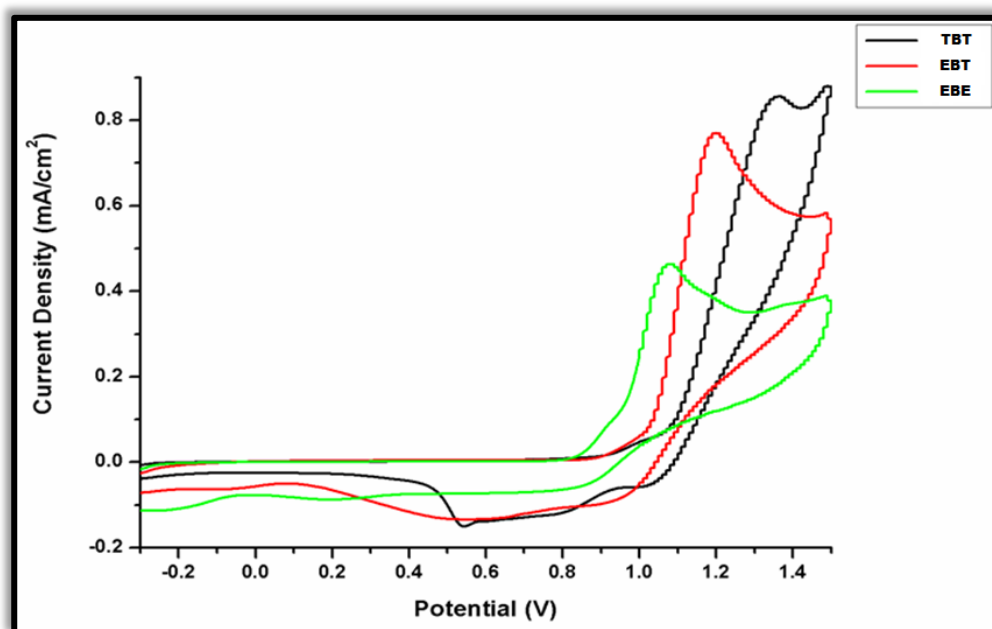


Figure 3.7 First cycles of TBT, EBE and EBT in 0.1 M DCM/ACN/TBAPF₆ solvent-electrolyte couple during electrochemical polymerization

Oxidation and reduction onset values were used to determine the band gap energies for PTBT, PEBE and PEBT since all the polymers are both p- and n-type dopable. As seen from Table 3.1, the LUMO levels of three polymers are the

same since benzothiadiazole was used as the common acceptor unit. However, as the donor strength increases the HOMO energy levels decrease due to the electron rich EDOT units incorporated into the polymer structure. Calculated optical and electrochemical band gap values for PTBT (1.65 eV), PEBE (1.1 eV) and PEBT (1.2 eV) are in good agreement confirming the identical electrochemical processes for both methods (CV and spectroelectrochemistry).

Table 3 1 Electronic and optical results for PTBT, PEBE and PEBT.

	E_m^{ox} (V)	E_p^{ox} (V)	E_p^{red} (V)	HOMO/LUMO (eV)	E_g^{op} (eV)	E_g^{el} (eV)
PTBT	1.36	1.09	0.61	-5.40/-3.75	1.5	1.65
PEBE	1.07	0.90	0.7	-4.85/-3.75	1.2	1.1
PEBT	1.2	1.06	0.85	-5.0/-3.75	1.18	1.25

Like all donor-acceptor-donor type polymers, PTBT, PEBE and PEBT have two absorption maxima, however only PEBE revealed green color owing to its π - π^* transitions placed at around 428 nm and 755 nm in its neutral state. PTBT has one transition at 560 nm whereas its second transition is not in the visible region. The normalized monomer and resulting polymer film absorptions of PTBT, PEBE and PEBT are shown in Figure 3.8. It is seen that when thiophene units were replaced by EDOT units, monomer absorbance values were shifted to lower energies. This trend was also observed in the absorbance values of polymer films. Also, since the conjugation length was increased, all dominant wavelengths were

shifted to right for polymers PTBT, PEBE and PEBT compare to the ones for their monomers.

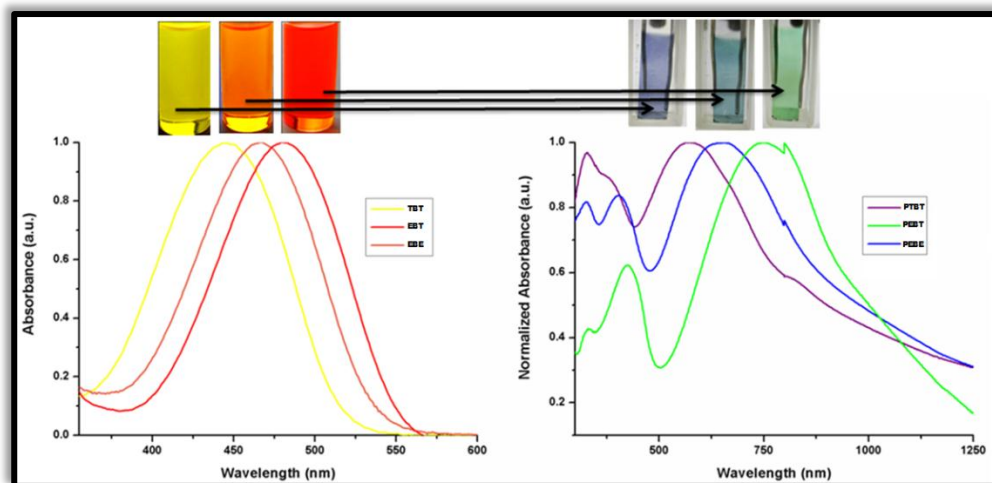


Figure 3.8 Electronic absorption spectra of monomers TBT, EBE and EBT (left) in CHCl₃ and polymers PTBT, PEBE and PEBT in thin film form (right).

3.1.3 Electronic and Optical Properties of Copolymers

3.1.3.1 Electrochemical Studies of Copolymers

Copolymerization studies were performed by using TBT and EBE as the co-monomers in order to investigate whether the resulting copolymers will have the same optical and electrical properties with P₃. Since EBT has both thiophene and EDOT units on its polymer backbone, its polymer PEBT may reveal the similar electrochemical and optical characteristics with the copolymers. During

potentiodynamic scans, two monomer oxidations were observed for TBT and EBE distinctively and reversible redox peaks were determined for the copolymers. Table 3.2 summarizes the monomer and polymer redox potentials for electrochemically prepared copolymers. As the amount of TBT increased in the feed, the polymer redox peaks were slightly shifted to higher potentials due to the increased amount of thiophene units on the polymer backbone. Likewise, PEPT showed similar electrochemical properties with those of the copolymers prepared from different feed ratios.

Table 3 2 Monomer oxidation and accompanied polymer redox potentials of copolymers prepared from co-monomers TBT and EBE.

Comonomer Composition		2TBT:1EBE	1TBT:1EBE	1TBT:2EBE	1TBT:4EBE	1TBT:10EBE
$E_{\text{mon}}^{\text{ox}}$ (V)	EBE	1.23	1.14	1.07	1.13	1.00
	TBT	1.42	1.38	1.35	1.40	1.40
$E_{\text{poly}}^{\text{ox}}$ (V)		1.34	1.30	1.28	1.28	1.26
$E_{\text{poly}}^{\text{red}}$ (V)		0.94	0.91	0.85	0.75	0.58

3.1.3.2 Spectroelectrochemical Studies of Copolymers and Comparison with Homopolymers

Figure 3.9 displays the normalized absorbance of each copolymer film in neutral state prepared from different compositions. PTBT, PEBE and PEBT demonstrate a clear shift in the dominant wavelength as the co-monomer composition is varied from pure PTBT to pure PEBE. As the concentration of EBE is increased in the copolymer chain, the π - π^* absorptions of the copolymers were shifted to lower energies from 391 nm to 422 nm and 596 nm to 724 nm. The observed red shift indicated a “tunable” electrochromic material can be synthesized by varying the amount of any monomer in the copolymer backbone.

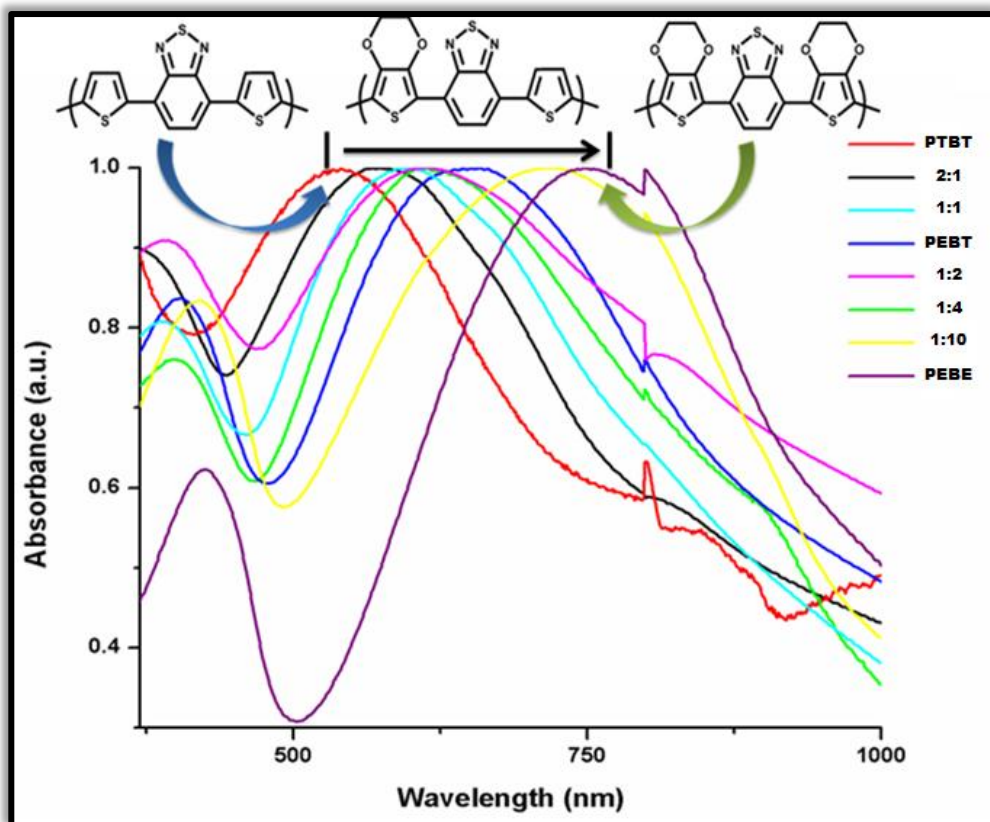


Figure 3.9 Normalized absorbance spectra of PTBT, PEBE, PEBT and the copolymer films prepared from different compositions (all in neutral state).

Here, it is noteworthy to emphasize that PEBT showed the electrochemical and optical properties of the copolymer (1:4, TBT:EBE ratio) hence PEBT can be used like a copolymer. Most of the copolymer studies in the literature state that the copolymerization of two co-monomers often results in a random copolymer. However, it can be achieved a controlled polymerization with similar properties to that of copolymers using TBT and EBE as the co-monomers. Table 3.3 summarizes λ_{\max} values and optical band gap energies for PTBT, PEBE, PEBT and the copolymers obtained from TBT and EBE, which is very similar to the one reported for the copolymer obtained using 1:4 TBT:EBE ratio.

Table 3 3 Maximum wavelength values and optical band gap energies of PTBT, PEBE, PEBT and resulting copolymers.

	TBT	2:1 TBT:EBE	1:1 TBT:EBE	1:2 TBT:EBE	1:4 TBT:EBE	EBT	1:10 TBT:EBE	EBE
Neutral State Colors								
λ_{\max} (nm)	- 560	384 574	391 596	395 613	404 619	408 642	422 724	428 755
E_g^{op} (eV)	1.5	1.41	1.36	1.06	1.18	1.18	1.2	1.2

3.2 Electrochemical and Optical Properties of Quinoxaline Derivative Polymers

3.2.1 Electrochemical and Optical Properties of PTQT and PEQT

3.2.1.1 Electrochemistry of PTQT and PEQT

TQT and EQT were polymerized potentiodynamically with applied potentials between 0 and 1.4 V and -0.2 and 1.3 V, respectively, versus Ag wire pseudo-reference electrode in a 0.1 M tetrabutylammonium hexafluorophosphate (TBAPF₆) and 1×10^{-2} monomer solution in dichloromethane/acetonitrile (5:95, v:v) onto indium tin oxide (ITO)-coated glass slides at a scan rate of 100 mV/s. In the Figure 3.10 the repetitive cycles with increasing current density reveal that both polymers were well adhered onto the ITO surface. The irreversible monomer oxidations were observed at 1.25 and 0.9 V for TQT and EQT, respectively.

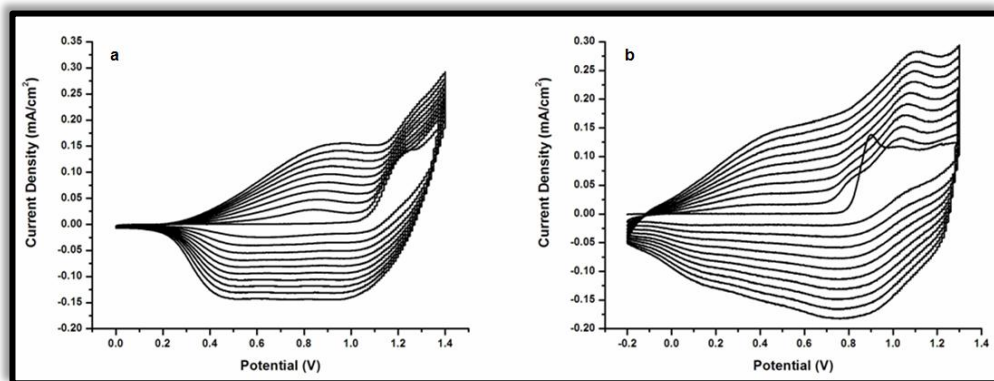


Figure 3.10 Electrochemical deposition of PTQT (a) and PEQT (b) on ITO-coated glass slide in a 0.1 M DCM/ACN/TBAPF₆ solvent–electrolyte couple.

The potential difference between the monomer oxidation peaks is related with the higher electron density on 3,4-ethylenedioxythiophene group than the thiophene group. Also, their monomer oxidations were higher than the one for EQE (0.8 V). This is due to the fact that they have lower electron density than EQE. Polymer redox couple was observed for PTQT at 0.96 V/0.8 V and for PEQT at 0.7 V/0.6 V. Current response versus scan rate graphs showed a linear relation that indicates both polymerization processes are not diffusion limited and redox couples are reversible as seen in Figure 3.11.

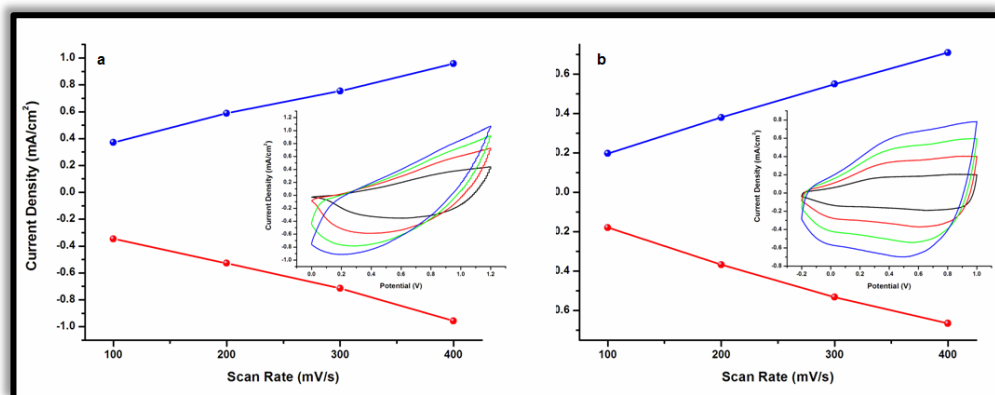


Figure 3.11 Scan rate dependence of PTQT (a) and PEQT (b) film for p-doping in 0.1 M ACN/TBAPF₆ solvent–electrolyte couple at 100, 200, 300, and 400 mV/s.

As other quinoxaline derivative polymers both PTQT and PEQT have n-doping properties at ambient conditions, which is a rare property in electrochromic polymers (Figure 3.12). Since both polymers are p- and n-type dopable, oxidation and reduction onset values were used to determine the bandgap energies. HOMO and LUMO energies were calculated against Fc/Fc⁺ reference electrode taking the

value of NHE as 4.75 eV versus vacuum. The HOMO/LUMO energy levels of PEQE were calculated from previously reported data.

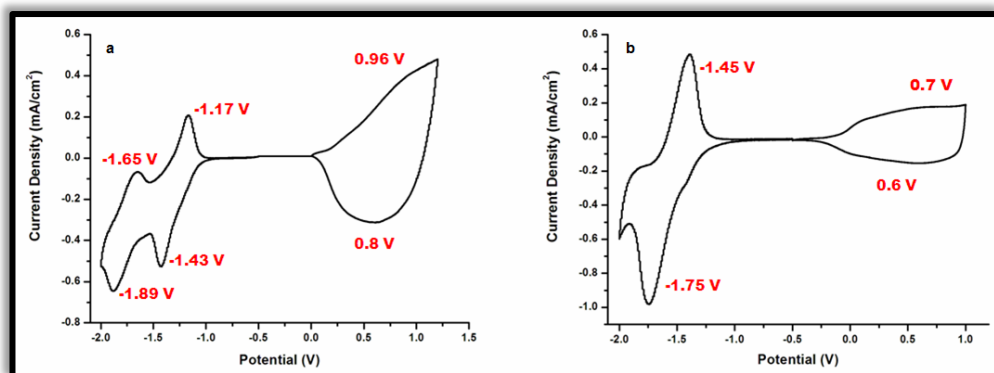


Figure 3.12 p- and n-type doping of PTQT (a) and PEQT (b) in 0.1 M ACN/TBAPF₆.

As seen from Table 3.4, the LUMO levels of three polymers are nearly the same since all contain quinoxaline as the acceptor unit. On the other hand, the HOMO energy levels were increased when the donor strength increased due to the incorporation of electron-rich 3,4-ethylenedioxy thiophene (EDOT) units into the polymer structure. Calculated optical and electrochemical bandgap values of the polymers indicate that this argument is valid as proven by both CV and spectroelectrochemistry studies.

Table 3 4 Monomer Oxidation, Corresponding Polymer Redox Potentials, Band Energies (HOMO/LUMO values), Optical and Electronic Bandgap Values of PTQT, PEQT, and PEQE

Polymer	E_{m}^{ox}	E_{p}^{ox}	E_{p}^{red}	E_{p}^{n-dope}	$E_{p}^{n-dedope}$	HOMO/LUMO	E_{g}^{op}	E_{g}^{el}
PTQT	1.25V	0.96V	0.8V	-1.43/- 1.89	-1.17/- 1.65	-5.25/-3.60 eV	1.55 eV	1.65 eV
PEQT	0.9V	0.7V	0.6V	-1.75V	-1.4V	-4.98/-3.65 eV	1.38 eV	1.33 eV
PEQE	0.8V	0.27V	0.08V	-1.7V	-1.45V	-4.75/-3.55 eV	1.18 eV	1.20 eV

3.2.1.2 Optical Studies of PTBPTQ and PTBPETQ

In their neutral state, PTQT revealed maximum absorption at 590 nm in the visible region, whereas its second transition maximum is not in the visible region resulting in a deep blue color for the polymer. On the other hand, both $\pi-\pi^*$ transitions are red shifted for PEQT, which have the maximum absorptions at around 400 and 690 nm revealing greenishblue color in the neutral state of the polymer as seen in Figure 3.13. To have a green color, there should be two transitions at around 400 and 700 nm in the visible region. The first $\pi-\pi^*$ transition of PTQT was seen in the UV region. On the other hand, the first $\pi-\pi^*$ transition of PEQT was seen at around 400 nm because of 3,4-ethylenedioxythiophene moiety. However, the second $\pi-\pi^*$ transition is at around 690 nm; hence, the polymer reveals greenish-blue color.

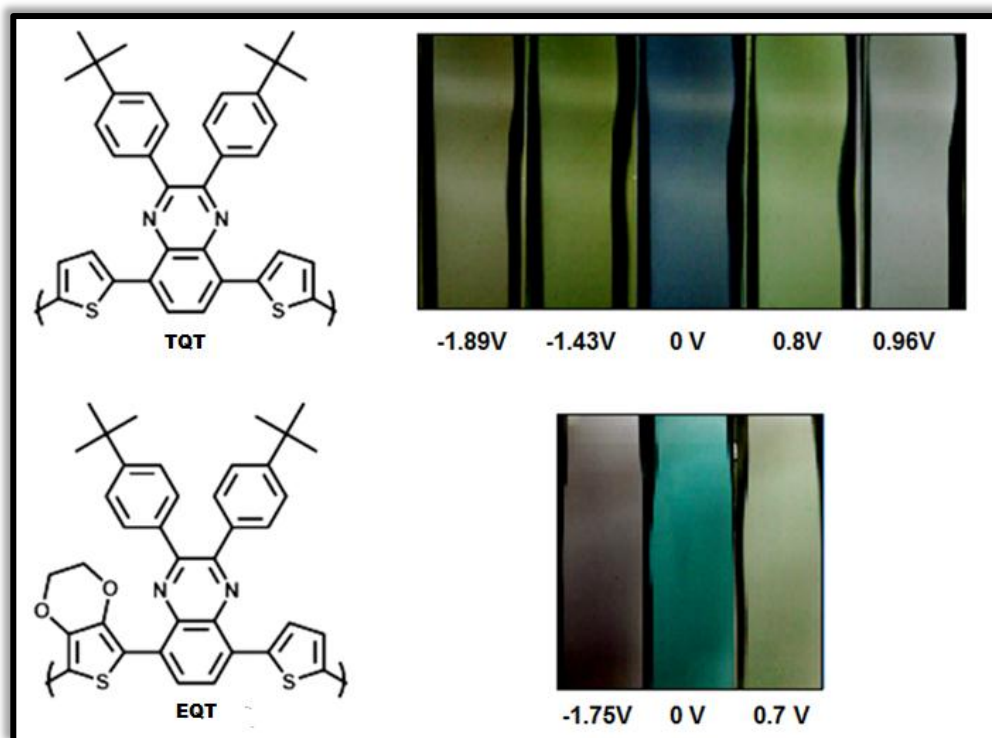


Figure 3.13 Chemical structures and colors of PTQT and PEQT at different potentials.

The normalized monomer and polymer film absorptions for PTQT, PEQT, and PEQE reveal that when thiophene groups were replaced by EDOT groups, monomer absorbance values and also polymer film absorbances were shifted to higher wavelengths due to the increase in electron density. Moreover, all dominant absorption wavelengths were shifted to red region for polymers PTQT, PEQT, and PEQE compared to the absorption wavelengths for their monomers because of the increased conjugation length as seen in Figure 3.14.

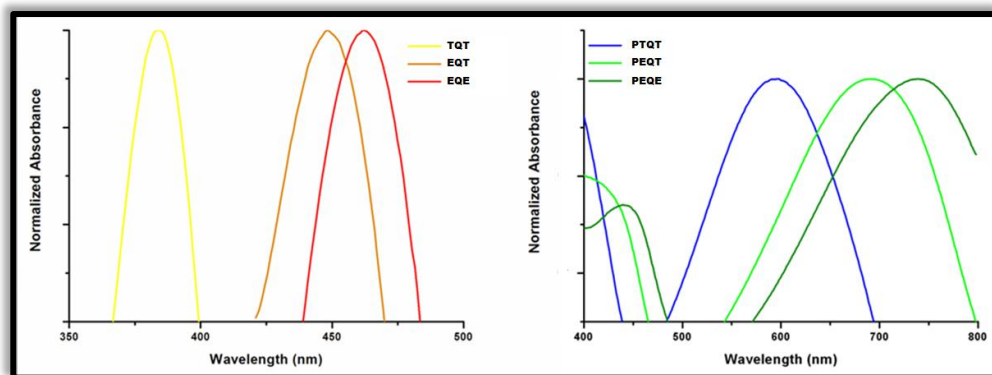


Figure 3.14 Electronic absorption spectra of monomers TQT, EQT, and EQE in DCM and polymers PTQT, PEQT, and PEQE in thin film form.

Their optical bandgap values were calculated from the onset of their second $\pi-\pi^*$ transitions as 1.55 eV for PTQT, 1.38 eV for PEQT, and 1.18 eV for PEQE. Spectral changes were recorded by UV-vis-NIR spectrophotometer in a monomer-free 0.1 M TBAPF₆/ACN solution while changing potentials between -0.3 and 1.5 V for PTQT and PEQT. In their neutral form, both polymers showed two transitions and no absorbance in NIR region. Upon p-type doping, formation of free charge carriers leads to new absorption bands at 830 and 1500 nm for PTQT and at 925 and 1800 nm for PEQT, whereas absorptions for the neutral state are decreasing (Figure 3.15). These new band formations represent the formation of polaron and bipolaron bands, respectively. Multichromic property was seen for the PTQT as the tail of the polaron band is in the visible region.

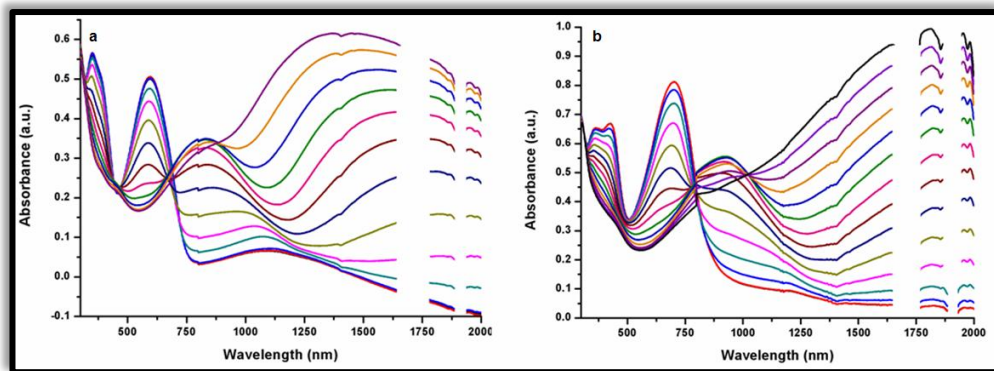


Figure 3.15 Electronic absorption spectra of PTQT (a) and PEQT (b) in 0.1 M ACN/TBAPF₆ system upon p-type doping.

For investigating optical contrast of polymers in thin film form, they were coated on ITO-coated glass. Potential was swept between their neutral and fully oxidized states to monitor the changes in transmittance as a function of time. The transmittance differences between the fully oxidized and reduced states of the polymers at different wavelengths were measured using a UV–vis–NIR spectrophotometer as the applied potential was switched between -0.3 and 1.3 V with a period of 5 s for both polymers. PTQT revealed 34 % optical contrast at 590 nm, 38 % at 830 nm, and 66 % at 1500 nm in Figure 3.16. The polymer film switches between the two states in 1 s (590 nm), 0.9 s (830 nm), and 0.3 s (1500 nm). PTQT shows competitive optical results compared with its EDOT-bearing homologs especially in NIR region. Although, PEQT exhibited lower optical contrast values in visible region compared to both PTQT and PEQE homologs due to its extant absorption at around 400 nm, it revealed promising optical contrast (64 %) in the NIR region.

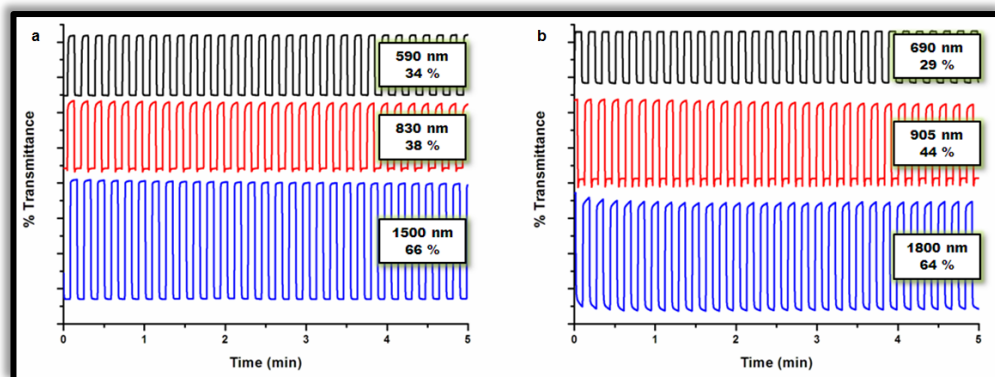


Figure 3.16 Optical transmittance changes of PTQT at 590, 830, and 1500 nm (a) and PEQT at 690, 905, and 1800 nm (b) in 0.1M ACN/TBAPF₆ system while switching the potentials between their neutral and oxidized states.

CHAPTER 4

CONCLUSION

In the first part of this study, an EDOT, thiophene and benzothiadiazole bearing donor–acceptor type monomer was synthesized and polymerized electrochemically as an alternative to copolymer studies. The polymer was characterized by electrochemically and optically. The resulting polymer is both p- and n-type dopable and showed the characteristics of a copolymer where two monomers are required. The results revealed that PEBT can be synthesized and its polymerization can be controlled to lessen the formation of a random copolymer. In the second part, two new quinoxaline derivatives bearing thiophene and 3,4-ethylenedioxythiophene units (TQT and EQT) were synthesized and potentiodynamically polymerized. The polymers were electrochemically and optically characterized. The resulting polymers are both p-and n-type dopable and showed high optical contrast in NIR region. Also, thiophene-bearing quinoxaline polymer (PTQT) revealed multichromic property, which is rare in electrochromic materials. When we compared the characterization results of the polymers with a previously synthesized quinoxaline derivative (PEQT), it was concluded that oxidation potential of both monomers and polymers increases as the electron density of the monomer/polymer decreases. Also, this decrease in the monomers/polymers leads to a blue shift in both monomer and polymer λ_{\max} values.

REFERENCES

- [1] H. Shirakawa, E. J. Louis, A. G. MacDiarmid, C. K. Chiang, A. J. Heeger, *J. Chem. Soc. Chem. Commun.*, **1977**, 578.
- [2] A. J. Heeger, *Angew. Chem. Int. Ed.*, **2001**, 2591.
- [3] C. K. Chiang, C. R. Fischer, Y. W. Park, A. J. Heeger, H. Shirakawa, E. J. Louis, S. C. Gau, A. G. MacDiarmid, *Phys. Rev. Lett.*, **1977**, 39, 1098.
- [4] A. O. Patil, A. J. Heeger, F. Wudl, *Chem. Rev.*, **1988**, 88, 183.
- [5] H. Letheby, *J. Chem. Soc.*, **1862**, 15, 161.
- [6] L. Groenendaal, F. Jonas, D. Freitag, H. Pielartzik, J. R. Reynolds, *Adv. Mater.*, **2000**, 12, 481.
- [7] H. B. Yildiz, L. Toppare, *Biosen. Bioelectron.*, **2006**, 2306.
- [8] D. Baran, A. Balan, S. Celebi, B. M. Esteban, H. Neugebauer, N. S. Sariciftci and L. Toppare, *Chem. Mater.*, **2010**, 22, 2978.
- [9] A. C. Grimsdale, K. L. Chan, R. E. Martin, P. G. Jokisz, A. B. Holmes, *Chem. Rev.*, **2009**, 109, 897.
- [10] S. Allard, M. Forster, B. Souharce, H. Thiem, U. Scherf, *Angew. Chem. Int. Ed.*, **2008**, 47, 4070.
- [11] G. Sonmez, *Chem. Commun.*, **2005**, 5251.
- [12] A. J. Heeger, *Chem. Soc. Rev.*, **2010**, 39, 2354.
- [13] S.F. Cogan, R.D. Rauh, J.D. Westwood, D.I. Plotkin, R.B. Jones, *Proc. SPIE*, **1989**, 1149, 2.
- [14] T. L. Rose, S. D'Antonio, M. H. Jillson, A. B. Kon, R. Suresh, F. Wang, *Synth. Metals*, **1997**, 85, 1439.
- [15] (a) S. K. Deb, *Appl. Opt., Suppl.* **1969**, 3, 192. (b) S. K. Deb, *Philos. Mag.*, **1973**, 27, 801.
- [16] R. G. Mortimer, *Chem. Soc. Rev.*, **1997**, 26, 147.
- [17] A. Pennisi, F. Simone, G. Barletta, G. Di Marco, L. Lanza, *Electrochimica Acta*, **1999**, 44, 3237.

- [18] D. R. Rosseinsky, R. J. Mortimer, *Adv. Mater.*, **2001**, 13, 783.
- [19] M. A. Habib, *Electrochem. Transition*, **1992**, 51.
- [20] P. R. Somani, S. Radhakrishnan, *Mater. Chem. Phys.*, **2003**, 77, 117.
- [21] F. C. Krebs, *Sol. Ener. Mat. Sol. Cells*, **2009**, 93, 394.
- [22] G. Sonmez, H. Meng and F. Wudl, *Chem. Mater.*, **2004**, 16, 574.
- [23] (a) G. Sonmez, C. K. F. Shen, Y. Rubin, F. Wudl, *Angew. Chem. Int. Ed.*, **2004**, 43, 1498. (b) I. Schwendeman, R. Hickman, G. Sonmez, P. Schottland, K. Zong, D. Welsh, J. R. Reynolds, *Chem. Mater.*, **2002**, 14, 3118. (c) H. S. Nalwa, *Handbook of Organic Conductive Molecules and Polymers*, John Wiley and Sons, New York, **1997**.
- [24] K. Fesser, A. R. Bishop, D. K. Campbell, *Phys. Rev. B*, **1983**, 27, 4804.
- [25] J. I. Reddinger, J. R. Reynolds, *Adv. Polym. Sci.*, **1999**, 45, 59.
- [26] J. Roncali, *Chem. Rev.*, **1997**, 97, 173.
- [27] J. L. Bredas, *J. Chem. Phys.*, **1985**, 82, 3806.
- [28] F. Wudl, M. Kobayashi, A. J. Heeger, *J. Org. Chem.*, **1984**, 49, 3382.
- [29] M. Pomerantz, B. Chalonnier-Gill, M. O. Harding, J. J. Tseng, W. J. Pomerantz, *Chem. Commun.*, **1992**, 1672.
- [30] J. L. Bredas, G. B. Street, B. Themans, J. M. Andre, *J. Chem. Phys.*, **1985**, 83, 1323.
- [31] S. Hotta, S. D. D. V. Rughooputh, A. J. Heeger, F. Wudl, *Macromol.*, **1987**, 20, 212.
- [32] (a) T. Yamamoto, Z. H. Zhou, T. Kanbara, M. Shimura, K. Kizu, T. Maruyama, Y. Nakamura, T. Fukuda, B. L. Lee, N. Ooba, S. Tomaru, T. Kurihara, T. Kaino, K. Kubota, S. Sasaki, *J. Am. Chem. Soc.*, **1996**, 118, 10389. (b) A. G. Agrawal, S. A. Jenekhe, H. Vanherzeele, J. S. Meth, *J. Phys. Chem.*, **1992**, 96, 2837.
- [33] C. A. Thomas, K. Zong, K. A. Abboud, P. J. Steel, J. R. Reynolds, *J. Am. Chem. Soc.*, **2004**, 126, 16440.
- [34] A. G. MacDiarmid, A. J. Heeger, *Synth. Met.*, **1979**, 1, 101.

- [35] M. Salmon, A. F. Diaz, A. J. Logan, M. Krounbi, J. Bargon, *J. Mol. Cryst. Liq. Cryst.*, **1983**, 83, 1297.
- [36] A. J. Heeger, S. Kivelson, J. R. Schrieffer, W. -P. Su, *Rev. Mod. Phys.*, **1988**, 60, 781.
- [37] D. Kumar, R. C. Sharma, *Eur. Polym. J.*, **1998**, 34, 1053.
- [38] G. Schopf, G. Kossmehl, *Adv. Polym. Sci.*, **1997**, 129, 166.
- [39] (a) R. J. Mortimer, A. L. Dyer, J. R. Reynolds, *Displays*, **2006**, 27, 2. (b) A. F. Diaz, A. Martinez, K. K. Kanazawa, M. M. Salmon, *J. Electroanal. Chem.*, **1981**, 130, 181.
- [40] K. Kaneto, Y. Kohno, K. Yoshino, Y. Inushi, *Chem. Commun.*, **1983**, 382.
- [41] R. F. Lane, A. T. Hubbard, *J. Phys. Chem.*, **1973**, 77, 1401.
- [42] O. Atwani, C. Baristiran, A. Erden, G. Sonmez, *Synth. Met.*, **2008**, 158, 83.
- [43] A. Durmus, G. E. Gunbas, P. Camurlu, L. Toppare, *Chem. Commun.*, **2007**, 3246.
- [44] G. E. Gunbas, A. Durmus, L. Toppare, *Adv. Mater.*, **2008**, 20, 691.
- [45] S. S. Zhu, T. M. Swager, *J. Am. Chem. Soc.*, **1997**, 119, 12568.
- [46] J. T. Pinhey, E. G. Roche, *J. Chem. Soc. Perkin Trans. 1*, **1988**, 2415.
- [47] C. M. Cardona, W. Li, A. E. Kaifer, D. Stockdale, G. C. Bazan, *Adv. Mater.*, **2011**, 23, 2367.
- [48] M. Sendur, A. Balan, D. Baran, B. Karabay, L. Toppare, *Org. Electron.*, **2010**, 11, 1877.
- [49] M. Sendur, A. Balan, D. Baran, L. Toppare, *J. Polym. Sci. Polym. Chem.*, **2011**, 49, 4065.

APPENDIX A

NMR DATA

Chemical shifts δ are reported in ppm relative to CHCl_3 (^1H : $\delta=7.27$), CDCl_3 (^{13}C : $\delta=77.0$) and CCl_4 (^{13}C : $\delta=96.4$) as internal standards.

^1H and ^{13}C NMR spectra of products are given below.

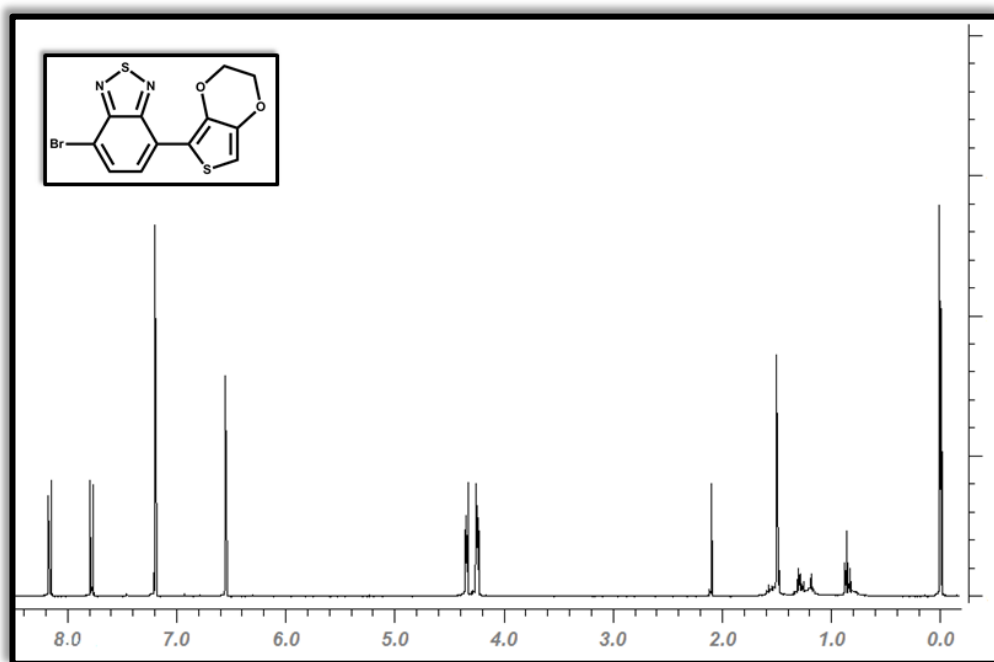


Figure A.1 ^1H NMR of 4-bromo-7-(2,3-dihydrothieno[3,4-b][1,4]dioxin-5-yl)benzo[c][1,2,5]thiadiazole

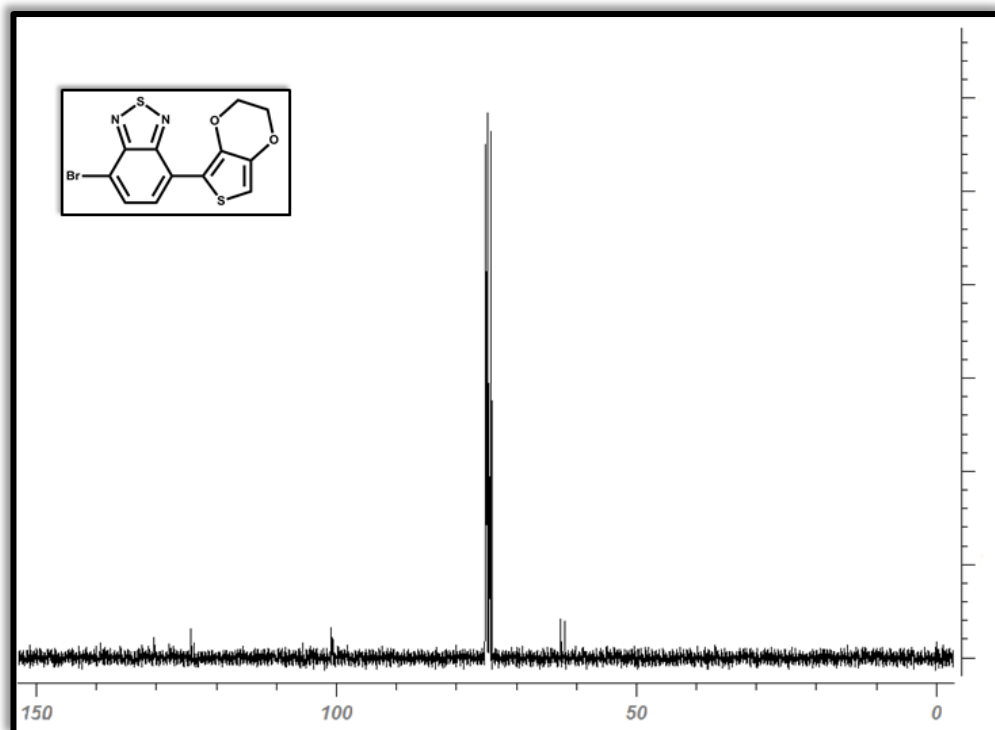


Figure A.2 ^{13}C NMR of 4-bromo-7-(2,3-dihydrothieno[3,4-b][1,4]dioxin-5-yl)benzo[c][1,2,5]thiadiazole

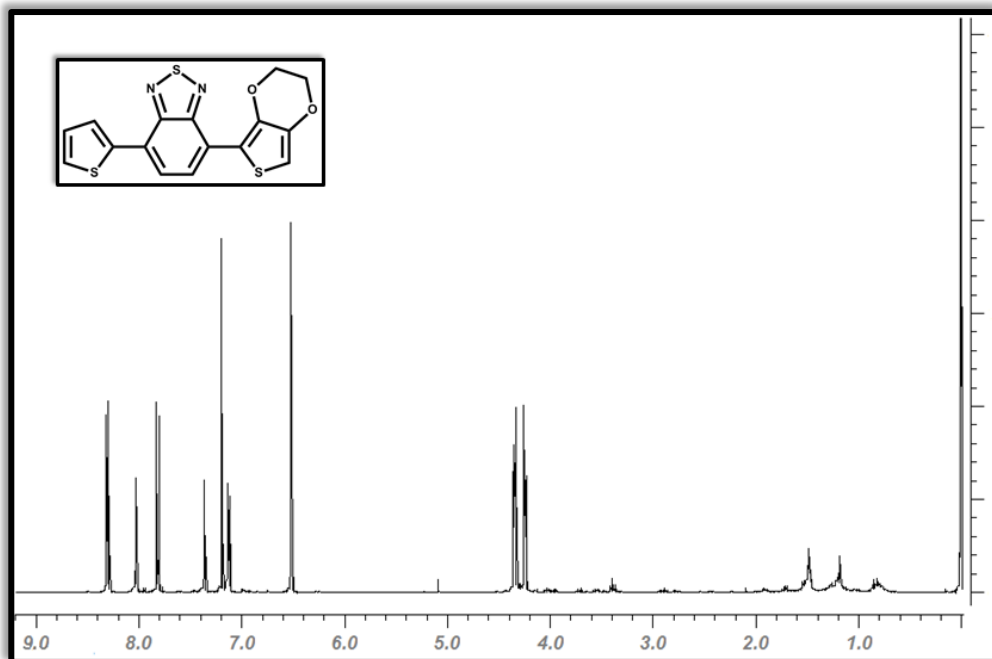


Figure A.3 ^1H NMR of EBT

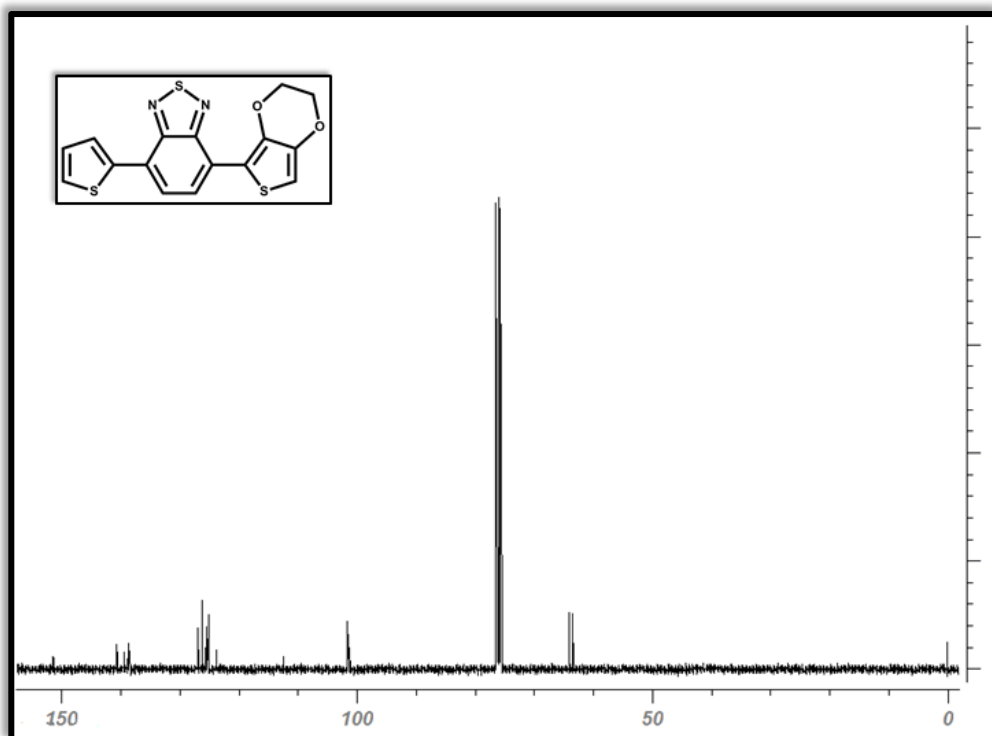


Figure A.4 ^{13}C NMR of EBT

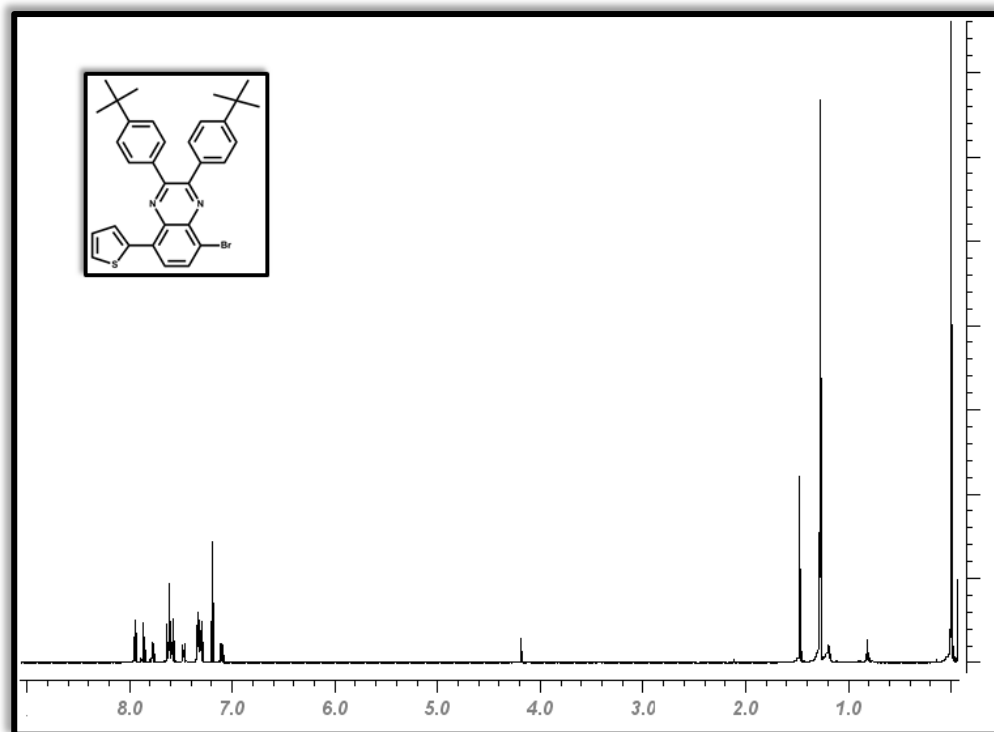


Figure A.5 ^1H NMR of Compound 1

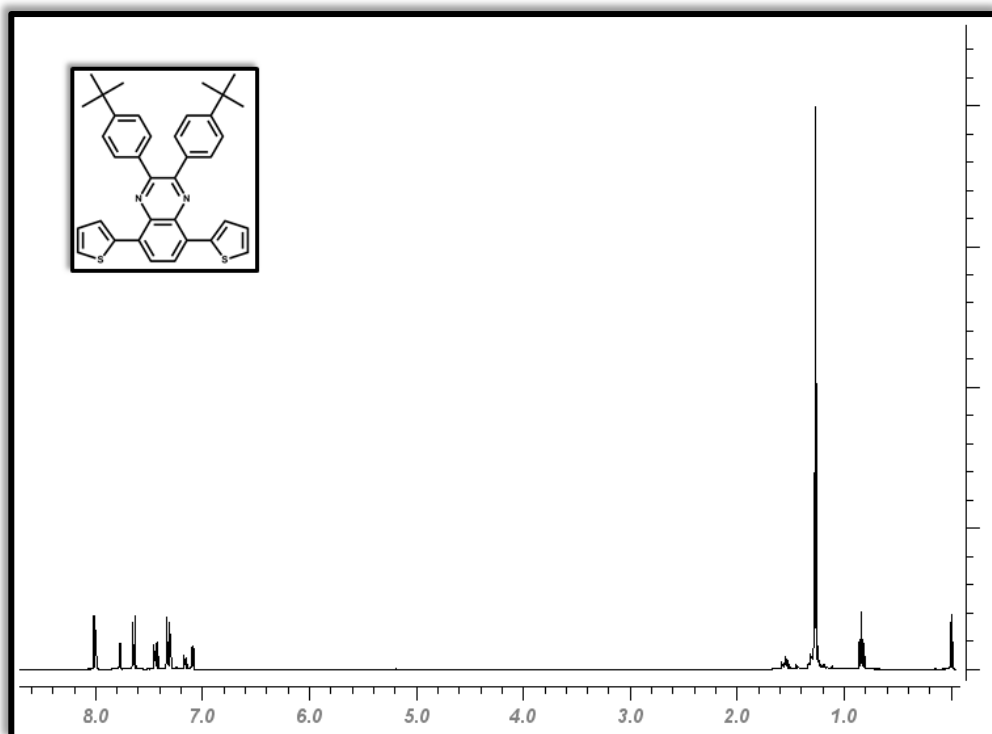


Figure A.6 ^1H NMR of TQT

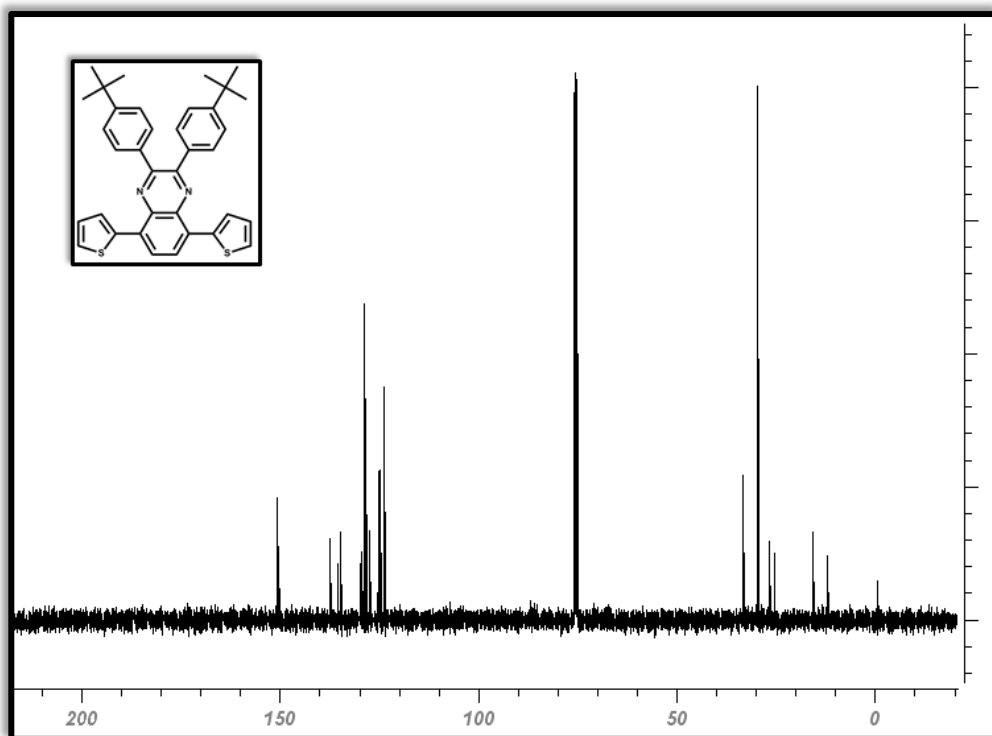


Figure A.7 ^{13}C NMR of TQT

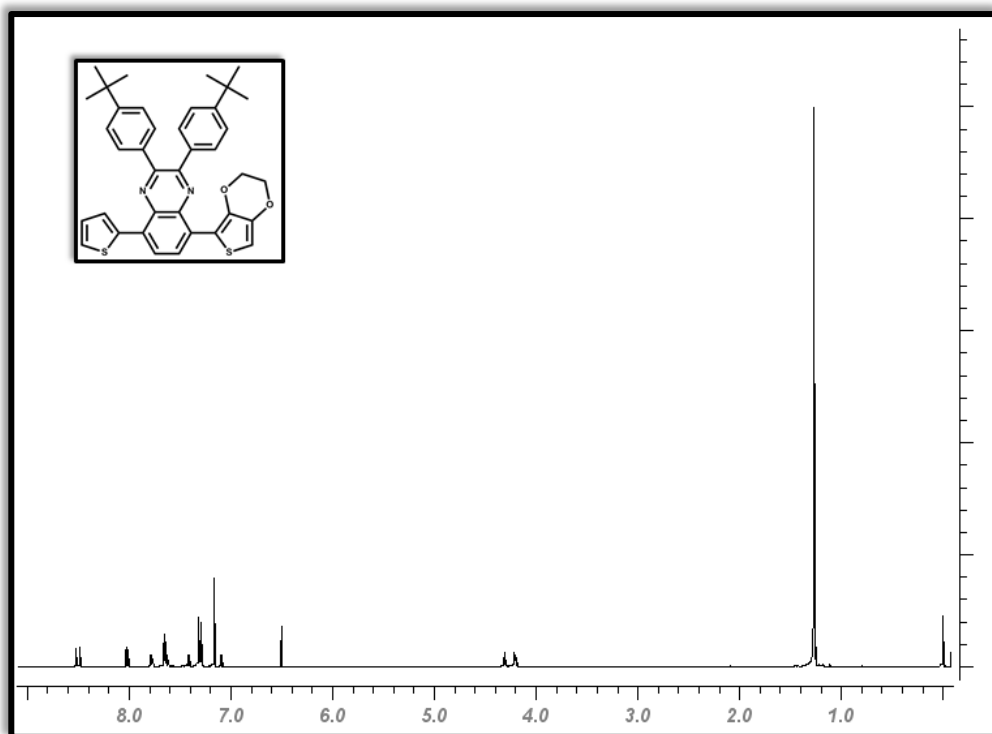


Figure A.8 ^1H NMR of EQT

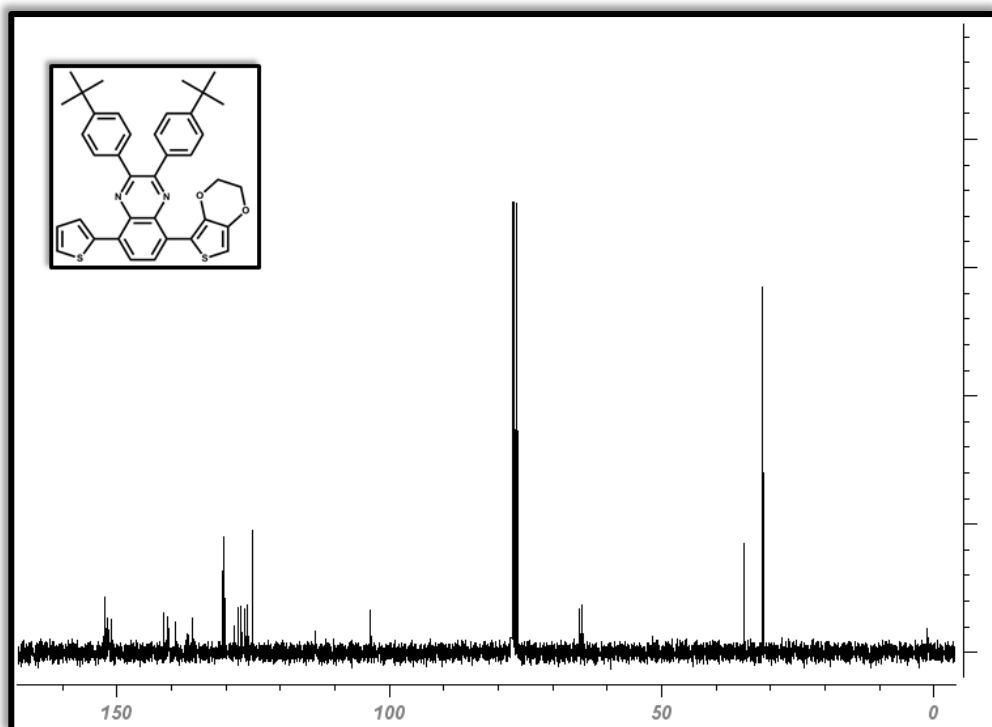


Figure A.9 ^{13}C NMR of EQT

APPENDIX B

HRMS DATA

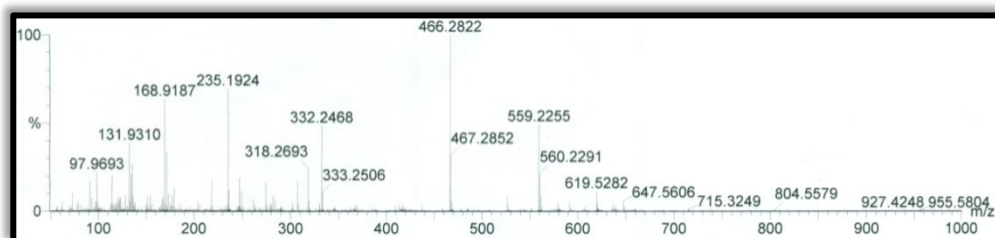


Figure A.10 HRMS of TQT

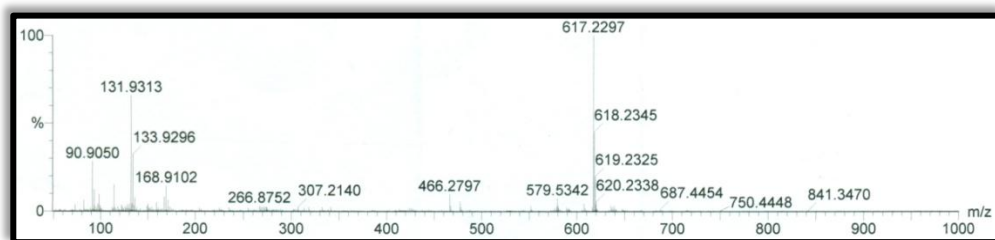


Figure A.11 HRMS of EQT

APPENDIX C

CYCLIC VOLTAMMOGRAMS OF COPOLYMERS

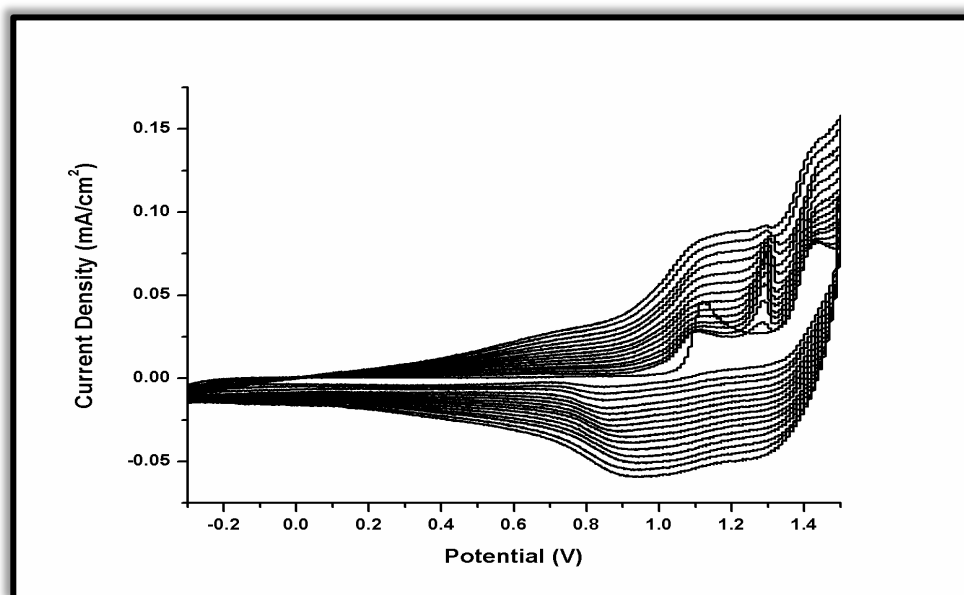


Figure A.12 CV of copolymerization with TBT:EBE; 2:1 monomer feed ratio.

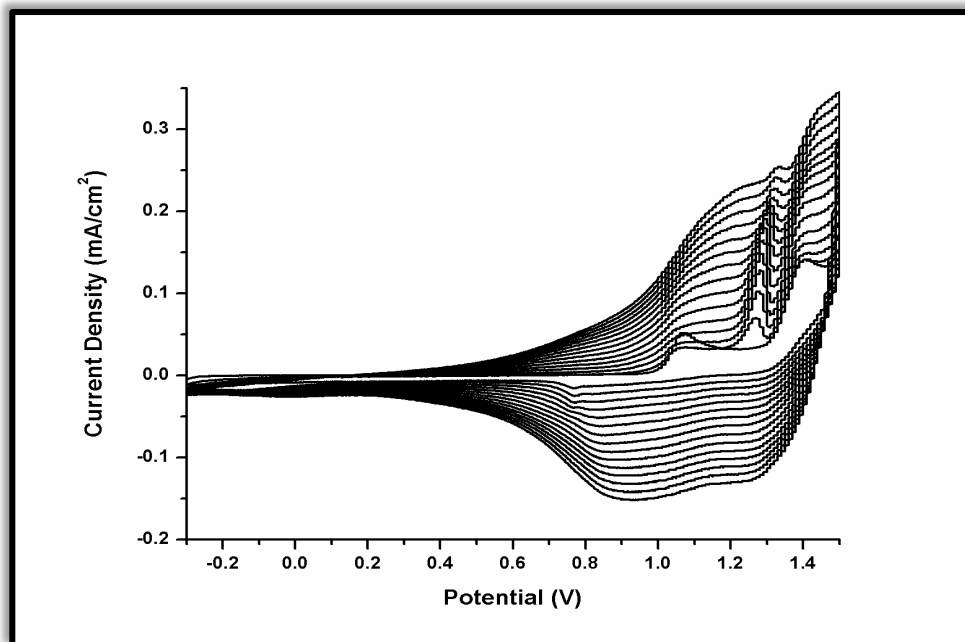


Figure A.13 CV of copolymerization with TBT:EBE; 1:1 monomer feed ratio.

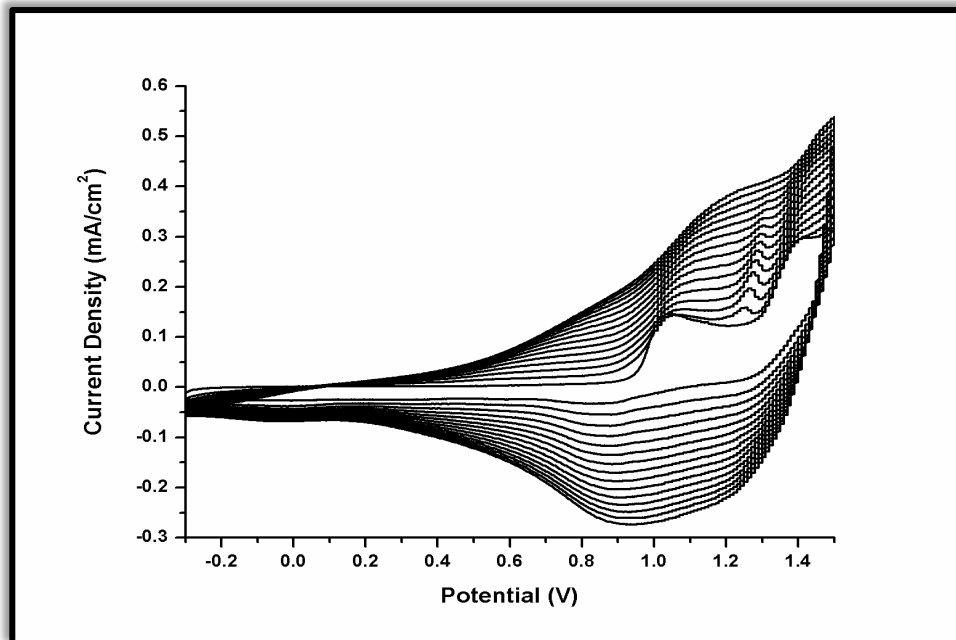


Figure A.14 CV of copolymerization with TBT:EBE; 1:2 monomer feed ratio.

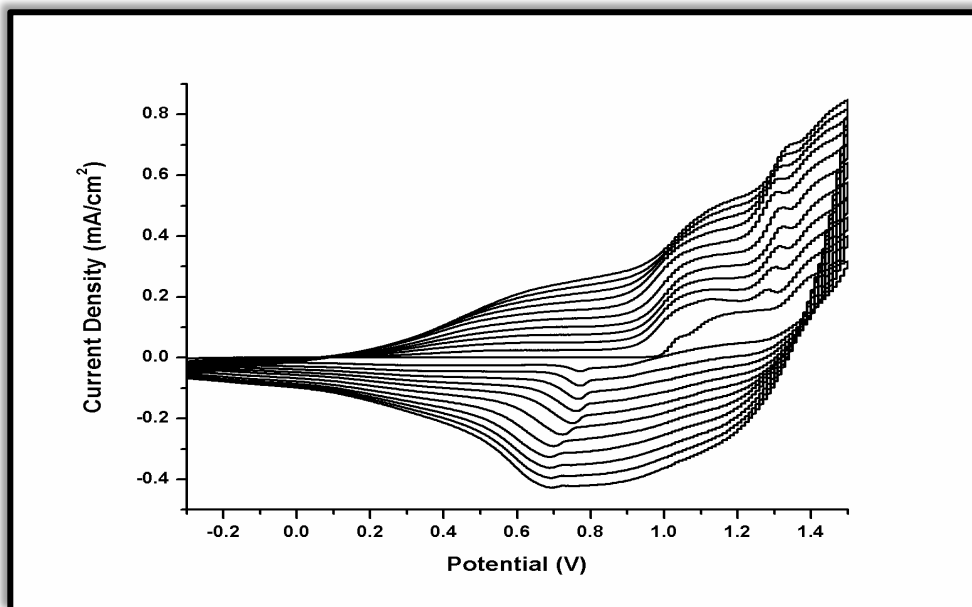


Figure A.15 CV of copolymerization with TBT:EBE; 1:4 monomer feed ratio.

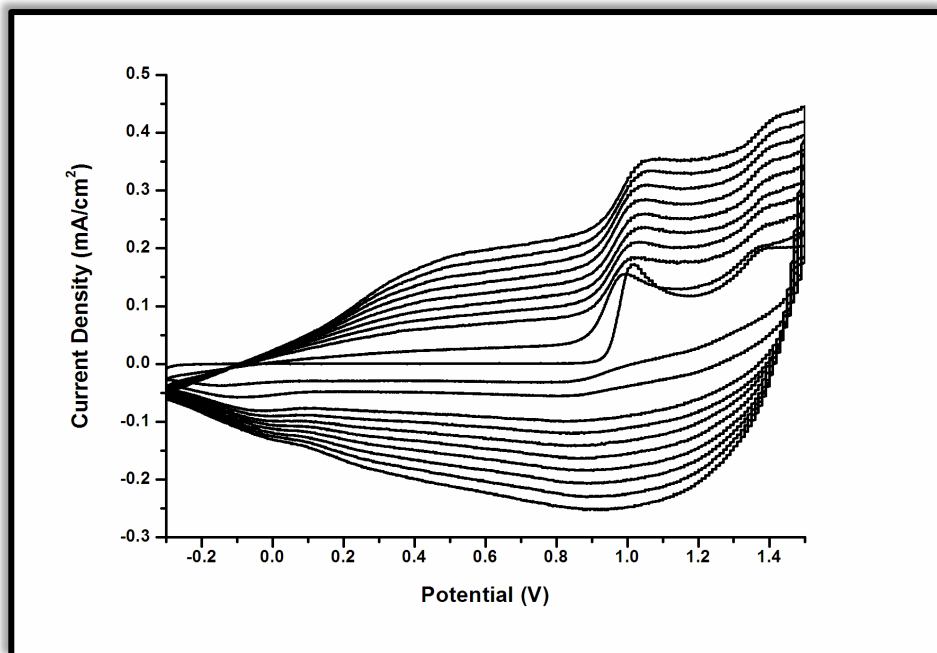


Figure A.16 CV of copolymerization with TBT:EBE; 1:10 monomer feed ratio.